Electroinduced two-nucleon knockout and correlations in nuclei

J. Ryckebusch [1], V. Van der Sluys, K. Heyde, H. Holvoet, W. Van Nespen and M. Waroquier

Department of Subatomic and Radiation Physics
University of Gent
Proeftuinstraat 86, B-9000 Gent, Belgium

M. Vanderhaeghen

CEA DAPNIA-SPhN, C.E. Saclay, France

Abstract

We present a model to calculate cross sections for electroinduced two-nucleon emission from finite nuclei. Short-range correlations in the wave functions and meson-exchange contributions to the photoabsorption process are implemented. Effects of the short-range correlations are studied with the aid of a perturbation expansion method with various choices of the Jastrow correlation function. The model is used to investigate the relative importance of the different reaction mechanisms contributing to the A(e,e′pn) and A(e,e′pp) process. Representative examples for the target nuclei ^{12}C and ^{16}O and for kinematical conditions accessible with contemporary high-duty cycle electron accelerators are presented. A procedure is outlined to calculate the two-nucleon knockout contribution to the semi-exclusive (e,e′p) cross section. Using this technique we investigate in how far semi-exclusive (e,e′p) reactions can be used to detect high-momentum components in the nuclear spectral function.

PACS : 24.10.-i,25.30.Rw,14.20.Gk
Keywords : electroinduced two-nucleon knockout, correlations

1 Introduction

The strong short-range and tensor component in realistic nucleon-nucleon interactions induces correlations in the nuclear many-body wave functions that

[1] E-mail : jan.ryckebusch@rug.ac.be

cannot be accounted for in an independent-particle approximation as for example adopted in the Hartree-Fock (HF) model. Over the years, various models that aim at going beyound the independent-particle model (IPM) wave functions, including effects of short-range and tensor correlations, have been proposed [1–5]. Despite the strongness of the tensor and short-range force it turns out to be a very challenging task to determine the proper measurable quantities that can verify the realistic character of those models. Cross sections for pion double-charge exchange reactions ${}_Z\mathrm{A}(\pi^+,\pi^-)_{Z+2}\mathrm{A}$ have been shown to exhibit some sensitivity to dynamical short-range correlations (SRC) but cannot yet distinguish between the different model predictions [6,7].

Better conditions to study the effects of correlations are predicted for reactions induced by leptonic probes. In contrast to pion-induced reactions, the data are not contaminated by effects related to initial-state interactions and the whole nuclear volume, including the interior, is sampled. It is believed that with the advent of a new generation of high-duty cycle electron facilities in the intermediate energy range ($\epsilon = 0.5 - 4$ GeV) good conditions have been created to explore the dynamics of ground-state correlations with unprecedented precision.

A key function in the study of ground-state correlations in nuclei is the single-particle spectral function $P(\vec{k}, E)$ that gives the probability to remove a nucleon with momentum $\vec{k}$ and find the residual A-1 system at an energy E. The most dramatic effects of the short-range and tensor correlations on $P(\vec{k}, E)$ are predicted to occur at high momentum and energy [8,9]. One should realize, however, that these parts of the spectral function belong to the smaller probability components in the nuclear wave functions. As a consequence, signals of ground-state correlations are likely to produce relatively small cross sections. This puts heavy constraints on the experimental requirements when performing measurements that aim at probing those correlations. Moreover, when exploring the small components in the nuclear wave functions one should start worrying about the role of competing mechanisms that could blur their effects in the actual cross sections. In this respect it is worth mentioning that the frequently quoted relation between the (e,e′p) cross section and the single-particle spectral function is based on rather severe assumptions regarding the reaction mechanism. Apart from the neglect of any sort of final-state interaction effect, the initial photoabsorption mechanism is assumed to be dominated by one-body operators. Even under quasi-elastic conditions, when this assumption is believed to have good chances to match reality, there are indications for many-body effects contributing to the (e,e′p) cross sections [10–12].

Already in the late fifties it was suggested that two-nucleon knockout reactions might shed some light on short-range correlations in nuclei. The underlying idea is that a photon hitting a strongly correlated nucleon pair will induce two nucleons to escape from the target [13]. Two-nucleon knockout reactions have

been extensively studied using real photons. In these investigations, data have been taken in a wide photon energy range ($E_\gamma < 1$ GeV), covering both the proton-proton and proton-neutron knockout channel. Rather than revealing information about ground-state correlations, the gross features of the (γ, pp) and (γ, pn) data could be interpreted in terms of meson-exchange and pion degrees of freedom [14–17]. Data for electroinduced two-nucleon knockout reactions are rather scarce. Pioneering experiments have been performed at NIKHEF-K [18,19]. More data will be collected at MAMI and TJNAF in the near future. It is hoped that the additional longitudinal degree of freedom will create optimum circumstances to reveal signatures of ground-state correlations.

One of the principal aims of this paper is to provide a framework in which models for ground-state correlations can be confronted with cross sections for electroinduced two-nucleon knockout reactions. In our developments we leave room for reaction mechanisms that can feed the two-nucleon knockout channel and cannot be directly associated with ground-state correlations. The major competing reaction mechanism consists of processes in which the photon is absorbed on two-, three-, ... nucleon currents. Just as the ground-state correlation effects these multi-body currents are a natural manifestation of the many-body dynamics of the nuclear system. For the present purposes we will restrict ourselves to two-body currents related to one-pion exchange. The framework in which those currents are treated, however, is rather general and can be extended to include the effects of heavier meson exchange. Apart from the exclusive two-nucleon knockout channel, we address also the (e,e′p) reaction. We concentrate on the high missing-energy region where the effects of ground-state correlations are predicted to manifest themselves. The exclusive nature of the electroproton reaction at high missing energies cannot be guaranteed. In our theoretical considerations, the starting point will be that the single-particle spectral function is not a directly measurable quantity. It will be argued that two-nucleon knockout represents an important fraction of the continuum (e,e′p) strength and that the (e,e′p) can be considered as a possible source of information about many-body dynamics in the nuclear system.

The outline of this paper is as follows. The specific ingredients of our model are introduced in Sec. 2. This includes a discussion of a practical way of calculating the exclusive (e,e′NN) (Sec. 2.1) and semi-inclusive (e,e′N) (Sec. 2.2) cross section. The model assumptions with respect to the meson-exchange and isobaric currents are outlined in Sec. 2.3 and those related to ground-state correlations in Sec. 2.4. The results of the (e,e′pp), (e,e′pn) and semi-inclusive (e,e′p) calculations are discussed in Sec. 3.

2 Formalism

2.1 The (e,e′NN) cross section

In the plane-wave approximation for the incoming and scattered electron waves the cross section for triple coincidence reactions of the type (e,e′$N_a N_b$) can be written as :

$$\frac{d^5\sigma}{dE_b d\Omega_b d\Omega_a d\epsilon' d\Omega_{\epsilon'}}(e,e'N_aN_b) = \frac{1}{4(2\pi)^8} k_a k_b E_a E_b f_{rec} \sigma_M$$
$$\times \Big[v_T W_T(\theta_a,\phi_a,\theta_b,\phi_b) + v_C W_L(\theta_a,\phi_a,\theta_b,\phi_b)$$
$$+ v_I W_{LT}(\theta_a,\phi_a,\theta_b,\phi_b) + v_S W_{TT}(\theta_a,\phi_a,\theta_b,\phi_b) \Big] , \quad (1)$$

where the Mott cross section σ_M is given by :

$$\sigma_M = \frac{e^2 cos^2\frac{\theta_e}{2}}{4\epsilon^2 sin^4\frac{\theta_e}{2}} . \quad (2)$$

For the cross section (1) we have considered the situation in which the residual $A-2$ nucleus is created at a fixed excitation energy E_x, which is expressed relative to its ground-state energy. As a consequence, the integration over the energy of one of the escaping particles has been performed. The functions v contain all the electron kinematics and read :

$$v_T = tg^2\frac{\theta_e}{2} - \frac{1}{2}\left(\frac{q_\mu q^\mu}{\vec{q}^2}\right) \quad (3)$$

$$v_C = \left(\frac{q_\mu}{\vec{q}}\right)^4 \quad (4)$$

$$v_I = \frac{q_\mu q^\mu}{\sqrt{2}\mid \vec{q}\mid^3}(\epsilon+\epsilon')tg\frac{\theta_e}{2} \quad (5)$$

$$v_S = \frac{q_\mu q^\mu}{2\vec{q}^2} . \quad (6)$$

The recoil factor in the above cross section reads :

$$f_{rec} = \frac{1}{1+\frac{E_a}{E_{A-2}}\left(1-\frac{qcos\theta_a}{k_a}+\frac{k_b cos\theta_{ab}}{k_a}\right)} , \quad (7)$$

where θ_{ab} is the angle between the directions of the ejected nucleons. The structure functions W are defined in terms of the electromagnetic transition operators between the ground state of the target nucleus and the final state and are functions of the polar (θ) and azimuthal (ϕ) angle of the two escaping

particles. Our choice for the reference frame and the notation conventions regarding the kinematical variables are summarized in Fig. A.1. In deriving the above expression we have not considered any polarization condition for the final products and the electrons. Accordingly, the structure functions W involve a sum over the spin projections (m_{s_a}, m_{s_b} and M_R) of the final products, including two escaping nucleons and a residual nucleus created in a specified state $\mid \Psi_f^{(A-2)}(E_x, J_R M_R) >$:

$$W_L(\theta_a, \phi_a, \theta_b, \phi_b) = \sum_{m_{s_a}, m_{s_b}, M_R} \Big(m_F^{fi}(\lambda = 0)\Big)^* \Big(m_F^{fi}(\lambda = 0)\Big) \tag{8}$$

$$W_T(\theta_a, \phi_a, \theta_b, \phi_b) = \sum_{m_{s_a}, m_{s_b}, M_R} \Big[\Big(m_F^{fi}(\lambda = +1)\Big)^* \Big(m_F^{fi}(\lambda = +1)\Big) + \Big(m_F^{fi}(\lambda = -1)\Big)^* \Big(m_F^{fi}(\lambda = -1)\Big)\Big] \tag{9}$$

$$W_{LT}(\theta_a, \phi_a, \theta_b, \phi_b) = 2Re\Bigg[\sum_{m_{s_a}, m_{s_b}, M_R} \Big[\Big(m_F^{fi}(\lambda = 0)\Big)^* \Big(m_F^{fi}(\lambda = -1)\Big) - \Big(m_F^{fi}(\lambda = 0)\Big)^* \Big(m_F^{fi}(\lambda = +1)\Big)\Big]\Bigg] \tag{10}$$

$$W_{TT}(\theta_a, \phi_a, \theta_b, \phi_b) = 2Re\Bigg[\sum_{m_{s_a}, m_{s_b}, M_R} \Big(m_F^{fi}(\lambda = -1)\Big)^* \times \Big(m_F^{fi}(\lambda = +1)\Big)\Bigg] , \tag{11}$$

with

$$m_F^{fi}(\lambda = \pm 1) = \Big\langle \Psi_f^{(A-2)}(E_x, J_R M_R); \vec{k}_a m_{s_a}; \vec{k}_b m_{s_b} \mid J_\lambda(\vec{q}) \mid \Psi_0 \Big\rangle \tag{12}$$

$$m_F^{fi}(\lambda = 0) = \Big\langle \Psi_f^{(A-2)}(E_x, J_R M_R); \vec{k}_a m_{s_a}; \vec{k}_b m_{s_b} \mid \rho(\vec{q}) \mid \Psi_0 \Big\rangle \ . \tag{13}$$

Here, $J_{\lambda=\pm 1}$ stands for the transverse components of the nuclear current density, ρ is the nuclear charge density and $\mid \Psi_0 >$ is the ground-state wave function of the target system. It goes without saying that computing the above matrix elements with a final state characterized by two scattering states can be very involving when accounting for the full complexity of the final-state interaction (FSI) and that several assumptions have to be made in order to keep the calculations feasible. In our model calculations we have put special emphasis on the orthogonality condition between the initial and final states thus avoiding spurious contributions entering the matrix elements. This is of particular importance in view of the fact that on several occasions we will make integrations over relatively large parts of the available phase space for the final products. In two-nucleon knockout from finite nuclei the final-state interaction involves apart from mutual interactions between the escaping nu-

cleons also distorting effects from the residual $A-2$ system. Another aspect of the FSI that deserves further attention is the role of multi-step processes. An obvious way to take these into account is a coupled-channel calculation. In the two-nucleon emission case, however, lots of channels are expected to contribute which makes a coupled-channel calculation very challenging. In the absence of a consistent and handleable theory to describe the full complexity of the FSI, we adopt the view that rather than accounting for only part of the FSI it is maybe better to work in a direct knockout model. Or put in other words, we assume that the two nucleons involved in the photoabsorption mechanism will escape from the target nucleus without being subject to inelastic collisions with the core. This is the basic assumption of the so-called "spectator approximation". In the shell-model picture, direct emission of two nucleons will leave the residual nucleus in a two-hole (2h) state relative to the ground state of the target nucleus. Even in a direct reaction model, the residual $A-2$ nucleons will distort the wave function of both escaping nucleons. In our model calculations this FSI effect is implemented along the lines explained in Ref. [20]. There it is shown that a proper A-body wave function with two asymptotically free nucleons and a residual nucleus generated in a 2h state can be reached by performing a partial wave expansion in terms of the two-hole-two-particle eigenstates of a mean-field one-body Hamiltonian. For the sake of completeness we mention the obtained expression for the required type of final wave function :

$$
\begin{aligned}
\mid \Psi_f > \equiv & \mid \Psi_f^{(A-2)}(E_x, J_R M_R); \vec{k}_a m_{s_a}; \vec{k}_b m_{s_b} > \\
= & \sum_{lm_l jm} \sum_{l' m_{l'} j' m'} \sum_{JMJ_1M_1} (4\pi)^2 i^{l+l'} \frac{\pi}{2M_N\sqrt{k_a k_b}} e^{i(\delta_l+\sigma_l+\delta_{l'}+\sigma_{l'})} \\
& \times Y^*_{lm_l}(\Omega_a) Y^*_{l'm_{l'}}(\Omega_b) < lm_l \frac{1}{2} m_{s_a} \mid jm >< jmj'm' \mid J_1M_1 > \\
& \times < l'm_{l'} \frac{1}{2} m_{s_b} \mid j'm' >< J_R M_R J_1 M_1 \mid JM > \\
& \times \mid (hh')^{-1} E_x J_R; (p(\epsilon_a lj) p'(\epsilon_b l'j')) J_1; JM > \ . \qquad (14)
\end{aligned}
$$

The model that we adopt to account for the FSI is thus based on a partial wave expansion in terms of two-hole-two-particle (2h2p) eigenstates of a mean-field potential. These wavefunctions are defined according to

$$
\begin{aligned}
& \mid (hh')^{-1} E_x J_R; (p(\epsilon_a lj) p'(\epsilon_b l'j')) J_1; JM >= \sum_{mm'} \sum_{M_1 M_R} \sum_{m_h m_{h'}} \frac{1}{\sqrt{1+\delta_{hh'}}} \\
& \times < jmj'm' \mid J_1M_1 >< J_R M_R J_1 M_1 \mid JM >< j_h m_h j_{h'} m_{h'} \mid J_R M_R > \\
& \times (-1)^{j_h+m_h+j_{h'}+m_{h'}} c^\dagger_{ljm} c^\dagger_{l'j'm'} c_{h-m_h} c_{h'-m_{h'}} \mid \Psi_0 > \ . \qquad (15)
\end{aligned}
$$

The continuum or particle (p) eigenstates of the mean-field potential are characterized by $p(\epsilon lj)$. The energy at which the partial waves $p(\epsilon lj)$ are calculated

is determined by the momentum of the emitted nucleon : $\epsilon^2 = k^2/(2M_N)$. The central and Coulomb phase shifts are denoted by δ_l and σ_l. Throughout this work we consider isospin not to be a good quantum number, in the sense that at the level of the single-particle states we discriminate between protons and neutrons. The single-particle wave functions are constructed through a Hartree-Fock calculation with an effective Skyrme type interaction [21]. For the protons a Coulomb part is added to the mean-field potential.

The state in which the final state is created is determined by $\mid (hh')^{-1} E_x J_R >$, with E_x the excitation energy with respect to the ground-state energy of the residual nucleus. A schematic drawing that illustrates the basic idea behind the expansion (14) is shown in Fig. A.2. It should be noted that in reality only a fraction of the final-state wave function will be of two-hole nature. Indeed, the many-body character of the residual system will make the two-hole strength to be fragmented over a wide energy range. In order to account for this nuclear structure effect, "spectroscopic factors" have to be considered when calculating cross sections for decay to specific states. The nuclear-structure aspects which are expected to play a role in the ^{16}O(e,e′pp) reaction have been the subject of a recent study reported in Ref. [22].

At a first sight, the usefulness of Eq. (14) is questionable as all expansions extend to infinity. When performing the calculations in coordinate space, finite expressions for the transition matrix elements can be obtained by performing an angular decomposition of the transition operators $(J_\lambda(q), \rho(q))$. This leads to the well-known expansion of the nuclear four-current operator in terms of the Coulomb (M^{coul}_{JM}), electric (T^{el}_{JM}) and magnetic (T^{mag}_{JM}) multipole operators ($\hat{J} \equiv \sqrt{2J+1}$)

$$J_{\pm 1}(q) = -\sqrt{2\pi} \sum_{J \geq 1} i^J \hat{J} \left(T^{el}_{J\pm 1}(q) \pm T^{mag}_{J\pm 1}(q) \right) \tag{16}$$

$$\rho(q) = \sqrt{4\pi} \sum_{J \geq 0} i^J \hat{J} M^{coul}_{J0}(q) \; . \tag{17}$$

After inserting the expansions for the final state (14) and the nuclear charge-current operator (16), the transition matrix elements of Eqs. (12) and (13) can be cast in the closed form :

$$\begin{aligned} m^{fi}_F(\lambda = \pm 1) = & -\sqrt{2\pi} \sum_{J \geq 1} i^J \hat{J} \sum_{l m_l j m} \sum_{l' m_{l'} j' m'} \sum_{J_1 M_1} \\ & \times (4\pi)^2 (-i)^{l+l'} \frac{\pi}{2M_N \sqrt{k_a k_b}} e^{-i(\delta_l + \sigma_l + \delta_{l'} + \sigma_{l'})} \\ & \times Y_{l m_l}(\Omega_a) Y_{l' m_{l'}}(\Omega_b) < l m_l \frac{1}{2} m_{s_a} \mid j m >< l' m_{l'} \frac{1}{2} m_{s_b} \mid j' m' > \end{aligned}$$

$$\times < jmj'm' \mid J_1M_1 > \frac{(-1)^{J_R-M_R+1}}{\hat{J}_1} < J_R - M_R J\lambda \mid J_1M_1 >$$
$$\times[\mathcal{M}^{el}_{pp';hh'}(J_1,J,J_R) + \lambda\mathcal{M}^{mag}_{pp';hh'}(J_1,J,J_R)] \tag{18}$$

$$m^{fi}_F(\lambda=0) = \sqrt{4\pi}\sum_{J\geq 0} i^J\hat{J}\sum_{lm_ljm}\sum_{l'm_{l'}j'm'}\sum_{J_1M_1}$$
$$\times(4\pi)^2(-i)^{l+l'}\frac{\pi}{2M_N\sqrt{k_ak_b}}e^{-i(\delta_l+\sigma_l+\delta_{l'}+\sigma_{l'})}$$
$$\times Y_{lm_l}(\Omega_a)Y_{l'm_{l'}}(\Omega_b) < lm_l\frac{1}{2}m_{s_a} \mid jm >< l'm_{l'}\frac{1}{2}m_{s_b} \mid j'm' >$$
$$\times < jmj'm' \mid J_1M_1 > \frac{(-1)^{J_R-M_R+1}}{\hat{J}_1} < J_R - M_R J0 \mid J_1M_1 >$$
$$\times\mathcal{M}^{coul}_{pp';hh'}(J_1,J,J_R)\ , \tag{19}$$

where the matrix elements $\mathcal{M}$ have been defined according to :

$$\mathcal{M}^{el,mag}_{pp';hh'}(J_1,J,J_R) =< p(\epsilon_b lj)p'(\epsilon_a l'j');J_1\|T^{el,mag}_J(q)\|hh';J_R >$$
$$-(-1)^{j_h+j_{h'}+J_R} < p(\epsilon_b lj)p'(\epsilon_a l'j');J_1\|T^{el,mag}_J(q)\|h'h;J_R >\ , \tag{20}$$
$$\mathcal{M}^{coul}_{pp';hh'}(J_1,J,J_R) =< p(\epsilon_b lj)p'(\epsilon_a l'j');J_1\|M^{coul}_J(q)\|hh';J_R >$$
$$-(-1)^{j_h+j_{h'}+J_R} < p(\epsilon_b lj)p'(\epsilon_a l'j');J_1\|M^{coul}_J(q)\|h'h;J_R >\ . \tag{21}$$

It should be stressed that the above expressions are general and that no assumption whatsoever regarding the nature of the inital photoabsorption mechanisms has been adopted. The contributing photoabsorption mechanisms will be discussed in Sects. 2.3 and 2.4.

2.2 The semi-exclusive (e,e′N) cross section

In comparison with exclusive (e,e′NN) reactions the semi-exclusive (e,e′p) channel is more attractive from the experimental point of view. For model calculations, however, the semi-exclusive channel can be more challenging than exclusive 2N knockout calculations. Indeed two-nucleon knockout is expected to feed the semi-exclusive (e,e′p) channel as soon as the thresholds are crossed. The calculation of the two-nucleon knockout contribution to the semi-exclusive channel involves integration over the phase space of the undetected escaping nucleon (either a proton or a neutron). In what follows we will exploit the fact that most of the derivations for the two-nucleon knockout cross sections in previous sections are done in coordinate space to perform some of these integrations analytically. In this way we facilitate the calculation of semi-exclusive

cross sections enormously and develop a framework that can be further exploited to investigate the role of the dynamical nucleon-nucleon correlations in the semi-exclusive channel. As most of the dynamical correlations are believed to be of two-body nature, one could expect that they manifest themselves most clearly in the two-nucleon emission channel. It is a major challenge to trace those kinematical regions where the semi-exclusive channel is predominantly fed by emission of two nucleons. Such investigations start from considering the contribution from (e,e′pp) and (e,e′pn) to the semi-exclusive channel :

$$\frac{d^4\sigma}{dE_p d\Omega_p d\epsilon' d\Omega_{\epsilon'}}(e,e'p) = \int d\Omega_{p'} \int dE_{p'} \frac{d^6\sigma}{dE_p d\Omega_p dE_{p'} d\Omega_{p'} d\epsilon' d\Omega_{\epsilon'}}(e,e'pp)$$
$$+ \int d\Omega_n \int dE_n \frac{d^6\sigma}{dE_p d\Omega_p dE_n d\Omega_n d\epsilon' d\Omega_{\epsilon'}}(e,e'pn) \; . \qquad (22)$$

An obvious way of determining the right-hand side of the above expression is calculating the 2N knockout cross sections for a grid of kinematical conditions that covers the full phase spaces $d\Omega_{p'}dE_{p'}$ ((e,e′pp) contribution) and $d\Omega_n dE_n$ ((e,e′pn) contribution). Those cross sections can then be integrated to obtain the semi-exclusive strength that is attributed to 2N knockout. Such a procedure would be cumbersome and would consume a lot a computing time. We present an alternative method that avoids those numerical integrations at a very small cost for the accuracy of the calculated cross sections. We start with remarking that most of the two-nucleon emission strength $\frac{d^6\sigma}{dE_p d\Omega_p dE_a d\Omega_a d\epsilon' d\Omega_{\epsilon'}}$ (a=p′,n) is confined to a relatively small fraction of the complete $d\Omega_a d\Omega_p$ phase space : ever since the original work by K. Gottfried [13] it has been clear that 2N knockout reactions predominantly occur in back-to-back situations (quasi-deuteron kinematics). Consequently, for a particular $dE_p d\Omega_p$ (semi-exclusive situation) most of the (e,e′ N_a p) strength will reside in a restricted angular range for the second nucleon N_a that remains undetected. In this restricted $d\Omega_a$ area the value of the undetected nucleon momentum, which is determined from energy-momentum conservation, will vary very slowly so that to a good approximation it can be replaced by an "average" value k_a^{ave}. This average momentum can be determined by imposing quasi-deuteron kinematics (which is equivalent with considering the situation with zero recoil momentum) :

$$\vec{q} - \vec{k}_a^{ave} - \vec{k}_p = \vec{0} \; , \qquad (23)$$

where $\vec{k}_p$ is the momentum of the detected proton. After introducing this "average momentum", the integration over $d\Omega_{p'}$ and $d\Omega_n$ in Eq. (22) can be performed analytically. Indeed, after inserting the expressions (18) and (19) into the structure functions $W(\theta_a, \phi_a, \theta_b, \phi_b)$ of Eqs. (8-11) it can be shown that :

$$\int d\Omega_a W_L(\theta_a,\phi_a,\theta_b,\phi_b) = \sum_{J,J'\geq 0}\sum_{lj}\sum_{l'j'}\sum_{l'_1j'_1}\sum_{J_1J'_1}\sum_{J_2}\sum_{hh'J_R}\frac{1}{1+\delta_{hh'}}\frac{64\pi^6}{M_N^2 k_a^{ave}k_b}$$
$$\times\mathcal{B}\left(p(k_a^{ave}lj),p'(k_bl'j'),p'_1(k_bl'_1j'_1),h,h',J_1,J,J'_1,J',J_R,J_2\right)$$
$$\times(-1)^{j+\frac{1}{2}+J_R+j'-j'_1+J_2}\left\langle J'\ 0\ J\ 0\mid J_2\ 0\right\rangle P_{J_2}\left(cos\theta_b\right)$$
$$\times\mathcal{M}^{coul}_{pp';hh'}(J_1,J,J_R)\left(\mathcal{M}^{coul}_{pp'_1;hh'}(J'_1,J',J_R)\right)^* \tag{24}$$

$$\int d\Omega_a W_T(\theta_a,\phi_a,\theta_b,\phi_b) = \sum_{J,J'\geq 1}\sum_{lj}\sum_{l'j'}\sum_{l'_1j'_1}\sum_{J_1J'_1}\sum_{J_2}\sum_{hh'J_R}\frac{1}{1+\delta_{hh'}}\frac{32\pi^6}{M_N^2 k_a^{ave}k_b}$$
$$\times\mathcal{B}\left[p(k_a^{ave}lj),p'(k_bl'j'),p'_1(k_bl'_1j'_1),h,h',J_1,J,J'_1,J',J_R,J_2\right]$$
$$\times(-1)^{j-\frac{1}{2}+J_R+j'-j'_1+J+J'}\left\langle J'\ -1\ J\ 1\mid J_2\ 0\right\rangle P_{J_2}\left(cos\theta_b\right)$$
$$\times\Big\{\Big[\mathcal{M}^{el}_{pp';hh'}(J_1,J,J_R)\left(\mathcal{M}^{el}_{pp'_1;hh'}(J'_1,J',J_R)\right)^*$$
$$+\mathcal{M}^{mag}_{pp';hh'}(J_1,J,J_R)\left(\mathcal{M}^{mag}_{pp'_1;hh'}(J'_1,J',J_R)\right)^*\Big]\times\left(1+(-1)^{J'+J+J_2}\right)$$
$$+\Big[\mathcal{M}^{el}_{pp';hh'}(J_1,J,J_R)\left(\mathcal{M}^{mag}_{pp'_1;hh'}(J'_1,J',J_R)\right)^*$$
$$+\mathcal{M}^{mag}_{pp';hh'}(J_1,J,J_R)\left(\mathcal{M}^{el}_{pp'_1;hh'}(J'_1,J',J_R)\right)^*\Big]\left(1+(-1)^{J'+J+J_2+1}\right)\Big\} \tag{25}$$

$$\int d\Omega_a W_{LT}(\theta_a,\phi_a,\theta_b,\phi_b) = \sum_{J\geq 1,J'\geq 0}\sum_{lj}\sum_{l'j'}\sum_{l'_1j'_1}\sum_{J_1J'_1}\sum_{J_2\geq 1}\sum_{hh'J_R}\frac{1}{1+\delta_{hh'}}\frac{64\sqrt{2}\pi^6}{M_N^2 k_a^{ave}k_b}$$
$$\times Re\Bigg[\mathcal{B}\left[p(k_a^{ave}lj),p'(k_bl'j'),p'_1(k_bl'_1j'_1),h,h',J_1,J,J'_1,J',J_R,J_2\right]$$
$$\times(-1)^{j_1+\frac{1}{2}+J_R+j'-j'_1+J_2}\left\langle J\ 1\ J'\ 0\mid J_2\ 1\right\rangle\frac{1}{\sqrt{J_2(J_2+1)}}P^1_{J_2}\left(cos\theta_b\right)$$
$$\times\Big\{\mathcal{M}^{el}_{pp';hh'}(J_1,J,J_R)\left(\mathcal{M}^{coul}_{pp'_1;hh'}(J'_1,J',J_R)\right)^*\left(e^{i\phi_b}+(-1)^{J+J'+J_2}e^{-i\phi_b}\right)$$
$$+\mathcal{M}^{mag}_{pp';hh'}(J_1,J,J_R)\left(\mathcal{M}^{coul}_{pp'_1;hh'}(J'_1,J',J_R)\right)^*$$
$$\times\left(e^{i\phi_b}+(-1)^{J+J'+J_2+1}e^{-i\phi_b}\right)\Big\}\Bigg] \tag{26}$$

$$\int d\Omega_a W_{TT}(\theta_a,\phi_a,\theta_b,\phi_b) = \sum_{J,J'\geq 1}\sum_{lj}\sum_{l'j'}\sum_{l'_1j'_1}\sum_{J_1J'_1}\sum_{J_2\geq 2}\sum_{hh'J_R}\frac{1}{1+\delta_{hh'}}\frac{32\pi^6}{M_N^2 k_a^{ave}k_b}$$
$$\times\mathcal{B}\left[p(k_a^{ave}lj),p'(k_bl'j'),p'_1(k_bl'_1j'_1),h,h',J_1,J,J'_1,J',J_R,J_2\right]$$
$$\times(-1)^{j-\frac{1}{2}+J_R+j'-j'_1+J_2}\left\langle J'\ 1\ J\ 1\mid J_2\ 2\right\rangle\frac{1}{\sqrt{(J_2-1)J_2(J_2+1)(J_2+2)}}P^2_{J_2}\left(cos\theta_b\right)$$
$$\times\Bigg[\Big[\mathcal{M}^{el}_{pp';hh'}(J_1,J,J_R)\left(\mathcal{M}^{el}_{pp'_1;hh'}(J'_1,J',J_R)\right)^*$$
$$-\mathcal{M}^{mag}_{pp';hh'}(J_1,J,J_R)\left(\mathcal{M}^{mag}_{pp'_1;hh'}(J'_1,J',J_R)\right)^*\Big]$$
$$\times\left(e^{-2i\phi_b}+(-1)^{(J_2+J'+J)}e^{2i\phi_b}\right)$$
$$-2Im\Big[\mathcal{M}^{mag}_{pp';hh'}(J_1,J,J_R)\left(\mathcal{M}^{el}_{pp'_1;hh'}(J'_1,J',J_R)\right)^*\Big]$$

$$\times \left(e^{-2i\phi_b} - (-1)^{(J_2+J'+J)} e^{2i\phi_b} \right) \Bigg] \,, \tag{27}$$

where the function $\mathcal{B}$ was defined according to :

$$\begin{aligned}
&\mathcal{B}\ [p(k_a l j), p'(k_b l' j'), p'_1(k_b l'_1 j'_1), h, h', J_1, J, J'_1, J', J_R, J_2] = \\
&\quad i^{J-J'+l'_1-l'} e^{-i\left(\delta_{l'}+\sigma_{l'}-\delta_{l'_1}-\sigma_{l'_1}\right)} \widehat{J}\widehat{J'}\widehat{j'}\widehat{j'_1}\widehat{J_1}\widehat{J'_1}\frac{1}{2}\left[1+(-1)^{(J_2+l'+l'_1)}\right] \\
&\quad \times \left\{ \begin{array}{cc} j' & j'_1 \ J_2 \\ J'_1 & J_1 \ j \end{array} \right\} \left\{ \begin{array}{cc} J_1 & J \ J_R \\ J' & J'_1 \ J_2 \end{array} \right\} \left\langle j' \frac{1}{2} j'_1 - \frac{1}{2} \mid J_2 0 \right\rangle
\end{aligned}$$

These expressions allow to compute directly the semi-exclusive cross sections as a function of the kinematical variables (θ_p, ϕ_p, T_p) without explicitly calculating the intermediate (e,e′NN) angular cross sections. In the actual calculations we account for the spreading of the two-hole strength in the energy spectrum of the A-2 system. This is done with the aid of a model explained in Ref. [23].

2.3 Meson-exchange and isobaric currents

In an independent-particle picture, the most direct source of two-nucleon knockout strength would be the coupling of the electromagnetic field to the hadronic two-body currents. These currents are mediated by the mesons which lie at the basis of the one-boson exchange picture of the nucleon-nucleon interaction. Here, we do not make any attempt to consider medium-corrections for the meson fields. In constructing the two-body currents, our starting point is the one-boson exchange (OBE) picture of the nucleon-nucleon interaction as it has been derived from nucleon-nucleon scattering data. The long-range part of the OBE potential is well established and dominated by pion exchange. In coordinate space it takes on the well-known form as a sum of a spin-spin and tensor interaction term [24]

$$\begin{aligned}
V_\pi(\vec{r}_{12}) = &\vec{\tau}_1.\vec{\tau}_2 \frac{1}{3} \left(\frac{f_{\pi NN}}{m_\pi} \right)^2 \\
&\times \left\{ \vec{\sigma}_1.\vec{\sigma}_2 + S_{12}(\hat{r}) \left[1 + \frac{3}{m_\pi r} + \frac{3}{(m_\pi r)^2} \right] \right\} \frac{e^{-m_\pi r}}{r} \,.
\end{aligned} \tag{28}$$

The current operator satisfying the continuity equation with this potential can be constructed from general field-theoretical methods. We have considered pseudovector πNN coupling and treated the two-body currents in the

non-relativistic limit [25]. This results in the well-known π-exchange current operators :

$$\vec{J}_\pi(\vec{q}_1,\vec{q}_2) = (-i)e\frac{f^2_{\pi NN}}{m^2_\pi}(\vec{\tau}_1\times\vec{\tau}_2)_3\left(\frac{\vec{\sigma}_1\,(\vec{\sigma}_2\cdot\vec{q}_2)}{\vec{q}_2^{\,2}+m^2_\pi} - \frac{\vec{\sigma}_2\,(\vec{\sigma}_1\cdot\vec{q}_1)}{\vec{q}_1^{\,2}+m^2_\pi} - \frac{(\vec{\sigma}_1\cdot\vec{q}_1)\,(\vec{\sigma}_2\cdot\vec{q}_2)}{(\vec{q}_1^{\,2}+m^2_\pi)\,(\vec{q}_2^{\,2}+m^2_\pi)}\,(\vec{q}_1-\vec{q}_2)\right)\,, \tag{29}$$

where the first two terms refer to the so-called Seagull current and the last term, which is quadratic in the pion propagators, to the pion-in-flight current.

In addition to the meson-exchange currents (MEC) derived from the OBE potential we have also considered processes in which nucleon excitations Δ_{33} are created (Fig. A.3). Here, the model dependency is intrinsically larger as the (transverse) currents cannot be constrained by the continuity equation. In order to construct the currents associated with Δ_{33} creation with subsequent pion exchange, we also rely on field-theoretical methods and adopt a non-relativistic approach. The $\pi N\Delta$ coupling is considered in the standard form :

$$\mathcal{L}_{\pi N\Delta} = \frac{f_{\pi N\Delta}}{m_\pi}\left(\vec{S}^\dagger.\vec{\nabla}\right)\left(\vec{T}^\dagger.\vec{\pi}\right)\,, \tag{30}$$

where $\vec{S}$ and $\vec{T}$ denote the spin and isospin $\frac{1}{2}\to\frac{3}{2}$ transition operators. In the $\gamma N\Delta$ coupling we retain solely the magnetic term

$$\mathcal{L}_{\gamma N\Delta} = F_\Delta(q^2_\mu)\frac{f_{\gamma N\Delta}}{m_\pi}\left(\vec{S}^\dagger\times\vec{\nabla}\right).\vec{A}\vec{T}^\dagger_3\,, \tag{31}$$

with $\vec{A}$ the external electromagnetic field and $F_\Delta(q^2_\mu)$ the electromagnetic form factor of the delta for which we used the standard dipole form. The (marginal) electric quadrupole term in the $\gamma N\Delta$ coupling is neglected throughout this work. With the above coupling lagrangians we arrive at the following expression for the Δ_{33}-current with π-exchange :

$$\begin{aligned}
\vec{J}_{\pi\Delta}(\vec{q},\vec{q}_1,\vec{q}_2) &= \frac{i}{9}\frac{f_{\gamma N\Delta}f_{\pi NN}f_{\pi N\Delta}}{m^3_\pi}F_\Delta(q^2_\mu)\\
&\times\left\{\left[G^{res}_\Delta+G^{non-res}_\Delta\right]\right.\\
&\quad\times\left[4\,(\vec{\tau}_2)_3\,(\vec{q}_2\times\vec{q})\,\frac{\vec{\sigma}_2\cdot\vec{q}_2}{\vec{q}_2^{\,2}+m^2_\pi}+4\,(\vec{\tau}_1)_3\,(\vec{q}_1\times\vec{q})\,\frac{\vec{\sigma}_1\cdot\vec{q}_1}{\vec{q}_1^{\,2}+m^2_\pi}\right.\\
&\quad\left.\left.+(\vec{\tau}_1\times\vec{\tau}_2)_3\left[(\vec{\sigma}_2\times\vec{q}_1)\,\frac{\vec{\sigma}_1\cdot\vec{q}_1}{\vec{q}_1^{\,2}+m^2_\pi}-(\vec{\sigma}_1\times\vec{q}_2)\,\frac{\vec{\sigma}_2\cdot\vec{q}_2}{\vec{q}_2^{\,2}+m^2_\pi}\right]\times\vec{q}\right]\right.
\end{aligned}$$

$$
\begin{aligned}
&+ \left[G_\Delta^{res} - G_\Delta^{non-res}\right] \\
&\quad \times \left[-2\,i\ (\vec{\tau}_2)_3\ ((\vec{\sigma}_1 \times \vec{q}_2) \times \vec{q})\,\frac{\vec{\sigma}_2 \cdot \vec{q}_2}{\vec{q_2}^{\,2} + m_\pi^2}\right. \\
&-2\,i\ (\vec{\tau}_1)_3\ ((\vec{\sigma}_2 \times \vec{q}_1) \times \vec{q})\,\frac{\vec{\sigma}_1 \cdot \vec{q}_1}{\vec{q_1}^{\,2} + m_\pi^2} \\
&\quad \left. - 2\,i\ (\vec{\tau}_1 \times \vec{\tau}_2)_3 \left[\vec{q}_2 \frac{\vec{\sigma}_2 \cdot \vec{q}_2}{\vec{q_2}^{\,2} + m_\pi^2} - \vec{q}_1 \frac{\vec{\sigma}_1 \cdot \vec{q}_1}{\vec{q_1}^{\,2} + m_\pi^2}\right] \times \vec{q}\right]\Bigg\} . \qquad (32)
\end{aligned}
$$

The $\pi N\Delta$ and $\gamma N\Delta$ coupling constants are taken from ref.[26] : ${f^2}_{\pi N\Delta}$ / $4\ \pi = 0.37$, $f_{\gamma N\Delta} = 0.12$. In the above expression for the isobaric current G_Δ^{res} denotes the Δ_{33} propagator for the resonant diagrams (Fig.A.3(a) and (c)). The corresponding propagator for the so-called non-resonant diagrams (Fig.A.3(b) and (d)) is denoted by $G_\Delta^{non-res}$. As we will consider energy transfers in the resonance region, special attention has been paid to constructing the Δ_{33} propagators. A free Δ_{33} excitation obtains a width through πN decay. The corresponding propagator would then read

$$
G_\Delta^{res} = \frac{1}{-E_\Delta^{res} + M_\Delta - \frac{i}{2}\Gamma_\Delta^{res}} , \qquad (33)
$$

where E_Δ^{res} is the intrinsically available energy for the resonance and the width Γ_Δ^{res} becomes [26,27]

$$
\Gamma_\Delta^{res} = \frac{2}{3}\frac{f_{\pi N\Delta}^2}{4\pi}\frac{\mid \vec{p}_\pi \mid^3}{m_\pi^2}\frac{M_N}{\sqrt{s}} , \qquad (34)
$$

where $\vec{p}_\pi$ is the decay momentum in the center-of-mass (c.o.m) frame of the πN system and $\sqrt{s}$ the total c.o.m. energy of the pion and nucleon. In the medium, however, the πN decay will be blocked by the Pauli principle. Various pion-nucleus [28], photoabsorption [29] and inclusive (e,e$'$) [30,31] experiments have pointed towards other strong medium modifications of the Δ_{33} resonance. Indeed, the inclusive A(e,e$'$) spectra show a pronounced broadening and damping of the resonance in comparison with A times the free electron nucleon cross section. It is common belief that this is mainly due to the coupling of the dominant $\Delta \to \pi N$ decay with the $\Delta N \to NN$ channel. It is precisely the latter channel which is under investigation in two-nucleon knockout experiments. The Δ-hole model [30] has been applied successfully to the description of inclusive (e,e$'$) reactions in the Δ_{33} resonance region [31]. In the Δ-hole model one adopts a dynamical description of isobar propagation in the nucleus. This results in a propagator of the form [30]

$$
G_\Delta^{res} = \frac{1}{-E_\Delta^{res} + M_\Delta - \frac{i}{2}\Gamma_\Delta^{res} + \delta W + W_\pi + W_{sp}} , \qquad (35)
$$

where δW accounts for Pauli blocking and W_π for coupling of the resonance to π^o and the nuclear ground state. These two terms tend to cancel each other so that W_{sp} will induce the major correction with respect to the free delta propagator of Eq. (33). The W_{sp} is a semi-phenomenological parametrization of the coupling of the delta with the more complicated channels. In the orginal formulation of the delta-hole model the W_{sp} was chosen to have a density-dependent central and spin-orbit part. Chen and Lee [32] have shown that an equally good description of the ^{12}C(e,e$'$) cross sections could be obtained by simply assuming that

$$W_{sp}[\mathrm{MeV}] = -30 - 40\ \mathrm{i}\ . \tag{36}$$

This prescription is in agreement with the results from recent total photoabsorption measurements [29] from which it was concluded that the Δ mass and width increases with growing nuclear density. The values for the Δ mass and width for ^{12}C quoted in Ref. [29] are in agreement with the above prescription. In what follows we will adopt the procedure (36) to account for the medium effects on the Δ_{33} propagation. Recently, this approach has been applied with some success to the description of the photonenergy dependence of the ^{12}C(γ,pp) and (γ,pn) cross sections in the resonance region [33].

It is well known that the delta peak in the inclusive (e,e$'$) cross section appears at a higher energy transfer ω than 300 MeV which is typical for real photon induced reactions. It is convenient to introduce the equivalent photon energy K to produce the same nuclear excitation energy as the virtual photon $(\vec{q},\omega)$

$$K = \omega + \frac{q_\mu q^\mu}{2M_N}\ . \tag{37}$$

A real photon with energy K produces the same πN c.o.m. energy as a virtual photon $(\vec{q},\omega)$.

As we are dealing with off-shell nucleons the photon energy is not completely available for internal excitation of the nucleon. As pointed out in Refs.[34,35] a reasonable substitution for E_Δ^{res} is :

$$(E_\Delta^{res})^2 = (M_N - \epsilon_h)^2 + 2K(M_N - \epsilon_h)\ , \tag{38}$$

where ϵ_h is the average binding energy of the nucleon on which the pion is reabsorbed. Remark that ϵ_h depends on the shell in which the nucleon is residing.

For the non-resonant diagrams (Fig.A.3(c) and (d)) the propagator becomes

$$G_{\Delta}^{non-res} = \frac{1}{-E_{\Delta}^{non-res} + M_{\Delta}} \ , \tag{39}$$

with

$$\left(E_{\Delta}^{non-res}\right) = \sqrt{\left(M_N + \frac{(T_a + T_b)}{2}\right)^2 + \mid \vec{q} \mid^2} - \omega \tag{40}$$

In the static limit (small ω and q), one obtains :

$$G_{\Delta}^{res} = G_{\Delta}^{non-res} = \frac{1}{M_{\Delta} - M_N} \ , \tag{41}$$

in which case the isobaric current operator of Eq. (32) reduces to the static operator form as e.g. derived in Ref.[36]. By no means the static limit should be considered realistic as soon as one is approaching equivalent photon energies K that probe the real resonance region.

In fitting nucleon-nucleon scattering data in terms of a particular One-Boson exchange potential it is a common procedure to regularize the πNN vertices for the finite size of the hadrons and the complexity of physical mechanisms that are thought to happen at distances which are short as compared with the average range of the pion. This is frequently done by introducing a monopole hadronic form factor.

$$\frac{\Lambda_{\pi}^2 - m_{\pi}^2}{\Lambda_{\pi}^2 + k^2} \tag{42}$$

at each πNN vertex. For the actual calculations, these hadronic form factors have also been introduced in the meson-exchange and isobaric current operators of Eqs. (29) and (32). Throughout this work, a pion cut-off mass Λ_{π} of 1250 MeV has been used [24].

2.4 Ground-state correlations

In all of the above considerations we have adopted the independent particle model (IPM) in which all nuclear wave functions are cast in a Slater determinant form. In this Subsection we present a method to impose corrections to that picture. To that purpose we rely on a perturbation expansion method [37,38] to calculate transition matrix elements between many-particle wave

functions that have been corrected for correlation effects that go beyond the IPM. Here, correlations in the nuclear wave functions are implemented via a technique inspired by the so-called correlated basis function (CBF) theory [39] in which correlated wave functions $\overline{\Psi}$ are derived from their (uncorrelated) independent particle limit through the operation of an operator $\widehat{\mathcal{G}}$. The latter corrects the Slater determinant Ψ for short-range and other correlations not accounted for in the IPM :

$$\mid \overline{\Psi}\rangle = \frac{\widehat{\mathcal{G}} \mid \Psi\rangle}{\sqrt{\left\langle \Psi \mid \widehat{\mathcal{G}}^{\dagger}\widehat{\mathcal{G}} \mid \Psi \right\rangle}} \ . \tag{43}$$

In the CBF theory, the operator $\widehat{\mathcal{G}}$ takes on the form of a symmetrized product of two-body correlation operators :

$$\widehat{\mathcal{G}} = \widehat{\mathcal{S}}\left[\prod_{i<j=1}^{A} \sum_{p=1,6} f_{ij}^{p}(\vec{r}_{ij}, \vec{R}_{ij}) \widehat{O}_{ij}^{p} \right] , \tag{44}$$

where $\vec{r}_{ij} = \vec{r}_i - \vec{r}_j$, $\vec{R}_{ij} = (\vec{r}_i + \vec{r}_j)/2$ and $\widehat{\mathcal{S}}$ is the symmetrization operator. The $\widehat{O}_{ij}^{p}$ are the isoscalar and isovector isospin operators of the scalar, spin and tensor type [40] :

$$\begin{aligned} \widehat{O}_{ij}^{p} \epsilon \{ & 1(p=1), \vec{\tau}_i \cdot \vec{\tau}_j (p=2), \vec{\sigma}_i \cdot \vec{\sigma}_j (p=3), \\ & \vec{\sigma}_i \cdot \vec{\sigma}_j \vec{\tau}_i \cdot \vec{\tau}_j (p=4), S_{ij}(p=5), S_{ij}\vec{\tau}_i \cdot \vec{\tau}_j (p=6) \} \ . \end{aligned} \tag{45}$$

The different components in the operator $\widehat{\mathcal{G}}$ reflect the fact that the nucleon-nucleon force is a function of the spin and isospin orientation of the interacting particles. Of all of the above components the central ($p = 1$) and tensor ($p = 6$) operator have been notified [5,41] to induce the largest correlation corrections to the nuclear Slater determinants obtained in the IPM approach.

Throughout this paper we will restrict ourselves to the effects induced by the central operator ($p = 1$), that induces short-range correlations (SRC) to the nuclear wave functions obtained in an IPM approach. It should be stressed, however, that the techniques expanded in this paper can also be applied to the other terms. In most of the calculations that address the correlation function $f_{ij}^{p=1}(\vec{r}_{ij}, \vec{R}_{ij})$ it is assumed that the functional dependence can be restricted to the relative coordinate of the interacting nucleon pair $r_{ij} =\mid \vec{r}_i - \vec{r}_j \mid$. This assumption, which considerably simplifies the calculation of the correlation functions, can be justified by considering that the range of the correlation function $f_{ij}^{p=1}$ is small with respect to the surface thickness of the nucleus. Accordingly, the dependence of $f_{ij}^{p=1}$ on the c.o.m. coordinate $\vec{R}_{ij}$ is anticipated

to be small. As a result of retaining solely the corrections induced by the short-range correlations, the correlated nuclear wave functions used throughout this paper read

$$\overline{\Psi}(\vec{x}_1, ..., \vec{x}_A) = \prod_{i<j=1}^{A} f_{ij}^{p=1}(r_{ij}) \Psi(\vec{x}_1, ..., \vec{x}_A)/\sqrt{N} \ , \tag{46}$$

where $\vec{x}$ is a shorthand notation for the radial and spin coordinates and N is the normalization factor

$$N = \int d\vec{x}_1 ....d\vec{x}_A \Psi^{\dagger}(\vec{x}_1, ..., \vec{x}_A) \left(\prod_{i<j=1}^{A} f_{ij}^{p=1}(r_{ij}) \right)^{*} \times \prod_{i<j=1}^{A} f_{ij}^{p=1}(r_{ij}) \Psi(\vec{x}_1, ..., \vec{x}_A) \tag{47}$$

Within the adopted assumptions an arbitrary transition matrix element between a correlated ground state $\mid \overline{\Psi}_o >$ and a final state $\mid \overline{\Psi}_f >$ can be rewritten as

$$\left\langle \overline{\Psi}_f \mid \widehat{O} \mid \overline{\Psi}_o \right\rangle \equiv \frac{1}{\sqrt{N_i N_f}} \left\langle \Psi_f \mid \widehat{O}^{eff} \mid \Psi_o \right\rangle \ , \tag{48}$$

with

$$\widehat{O}^{eff} = \prod_{i<j=1}^{A} (1 - g(r_{ij}))^{\dagger} \, \widehat{O} \prod_{k<l=1}^{A} (1 - g(r_{kl})) \ , \tag{49}$$

where we have introduced the central correlation function g which is defined according to $g(r_{ij}) = 1 - f_{ij}^{p=1}(r_{ij})$. In the absence of short-range corrections the correlation function $g(r_{ij})$ would simply be zero. The effective operator approach as formally written in Eq. (48) has the marked advantage that we can rely on standard techniques, like second quantization, when calculating the transition matrix elements between correlated many-body states. The adopted approach also allows to put the short-range correlations on the same footing as other mechanisms that can feed the electroinduced two-nucleon knockout channel. In this way it will become easier to evaluate the sensitivity of the calcaluted cross sections to the SRC relative to the other mechanisms. The effective operator of Eq. (49) is an A-body operator which makes the exact calculation of "correlated" transition matrix elements of the type (48) not feasible. Various cluster expansions, however, have been developed to approximate the matrix elements of Eq. (48) [38,42]. These techniques usually address matrix elements of the type $< \overline{\Psi}_o \mid \widehat{O} \mid \overline{\Psi}_o >$, where $\overline{\Psi}_o$ is the correlated ground state

of the nuclear system. Here, we are facing a quite different situation in the sense that we are dealing with transition matrix elements between wave functions of totally different origin, namely $\overline{\Psi}_o$ and a final state with two nucleons residing in the continuum. Given that two-nucleon knockout calculations are already quite cumbersome in a pure IPM, there is a practical limitation on the number of terms in the cluster expansion that can be accounted for. This does not necessarily mean, however, that the main effects of the SRC cannot be calculated to a high degree of accuracy. Most of the cluster expansion techniques developed for the calculation of the "correlated" matrix elements rely on an expansion into the different orders of the central correlation function g. Here, we will restrict ourselves to the terms linear in the correlation function g. Higher order terms require three and more correlated nucleons. Given that the central correlation effect is very short ranged, this type of multi-nucleon correlations could be expected to be less important than two-body correlations at normal nuclear densities. In all forthcoming derivations we assume that the transition operator $\widehat{O}$ in expression (48) has a one- and two-body part :

$$\widehat{O} = \sum_i \widehat{O}^{[1]}(i) + \sum_{i<j} \widehat{O}^{[2]}(i,j) \; . \tag{50}$$

Within the adopted assumptions the effective transition operator can then be written as :

$$\begin{aligned}
\widehat{O}^{eff} = & \sum_i \widehat{O}^{[1]}(i) + \sum_{i<j} \widehat{O}^{[2]}(i,j) - \sum_{i<j} \Big[\widehat{O}^{[1]}(i) + \widehat{O}^{[1]}(j) \Big] g(r_{ij}) \\
& - \sum_{i<j<k} \Big[\widehat{O}^{[1]}(i) g(r_{jk}) + \widehat{O}^{[1]}(j) g(r_{ik}) + \widehat{O}^{[1]}(k) g(r_{ij}) \Big] \\
& - \sum_{i<j} \widehat{O}^{[2]}(i,j) g(r_{ij}) \\
& - \sum_{i<j<k} \Big[\widehat{O}^{[2]}(i,j) g(r_{ik}) + \widehat{O}^{[2]}(i,j) g(r_{jk}) + \widehat{O}^{[2]}(i,k) g(r_{ij}) \\
& + \widehat{O}^{[2]}(i,k) g(r_{jk}) + \widehat{O}^{[2]}(j,k) g(r_{ij}) + \widehat{O}^{[2]}(j,k) g(r_{ik}) \Big] \\
& - \sum_{i<j<k<l} \Big[\widehat{O}^{[2]}(i,j) g(r_{kl}) + \widehat{O}^{[2]}(i,k) g(r_{jl}) + \widehat{O}^{[2]}(i,l) g(r_{jk}) \\
& + \widehat{O}^{[2]}(j,k) g(r_{il}) + \widehat{O}^{[2]}(j,l) g(r_{ik}) + \widehat{O}^{[2]}(k,l) g(r_{ij}) \Big] \; .
\end{aligned} \tag{51}$$

For the sake of brevity we did not write the terms in $g^\dagger$, that refer to final-state correlations, in the above expression. Formally these contributions have exactly the same form as the terms generated by the initial-state correlations. The above expression clearly illustrates how the short-range effects are put on the same footing as the other contributions in the photoabsorption mechanism. The effective transition operator has apart from the terms occuring

in the"original" operator $\widehat{O}$ additional terms that depend on the correlation function g. The implications of those terms for the two-nucleon knockout reaction have been illustrated in Fig. A.4. In the absence of correlations that go beyond the IPM only diagrams of the type (a) would contribute to a direct two-nucleon emission process. Diagram (a) corresponds with a genuine two-body absorption process as e.g. encountered in the situation in which a photon is coupled to a charged meson exchanged between two nucleons moving in a mean-field orbital. Diagram (d) is of the same form as diagram (a) and can be interpreted as a short-range correction to the two-body current contributions from diagram (a). It will introduce a decreased probability at short internucleon distances for two-body photoabsorption processes to occur. As those short-range events are already heavily cut by the introduction of hadronic form factors they have a rather small impact on the calculated cross sections [43].

Diagrams (c),(e) and (f) are typical events that are linear in the correlation function g and involve three and four-body operators. Given the numerical complexity of two-nucleon knockout calculations we will restrict ourselves to the two-body operators that arise from diagrams of the type (a) and (b). This is often referred to as the Single-Pair Approximation (SPA). Within the SPA, one retains those terms from the above expansion that refer to processes in which the photon hits two correlated nucleons as a result of which they are emitted from the target nucleus. In the calculations we do not account for reactions in which the photon couples to a nucleon as a result of which one (or two) nucleons in the recoiling (A-1) system are emitted. Moreover, we did not consider the final state correlations. Indeed, within the context of the SPA inclusion of the final state correlations would mean that one considers the correlation between two nucleons residing in a scattering state. This type of correlation could be expected to be small. To the best of our knowledge, no calculations are available that address the correlation function for the continuum states appearing in the final state of the reactions under study. Most investigations into the correlation function have solely addressed the nuclear ground state.

It is worth stressing that in the absence of ground-state correlations the one-body photoabsorption operator $\widehat{O}^{[1]}$ would not contribute to the direct dinucleon emission process. It is only after introducing the central (or Jastrow) correlations that it starts contributing and can be formally treated like e.g. the MEC. Referring to Eq. (51) it seems technically possible to write down effective many-body currents that arise from combining one-body photoabsorption and ground-state correlation effects. In the SPA, the effective two-body current that accounts for the short-range corrections in the ground state reads

$$\vec{J}^{[2]}_{SRC}(i,j) = -\left(\vec{J}^{[1]}(i) + \vec{J}^{[1]}(j)\right) g(r_{ij}) \; . \tag{52}$$

For the one-body current $\vec{J}^{[1]}$ we consider the standard form of the Impulse Approximation (IA) that has a convection and magnetization part. Consequently,

$$\begin{aligned}\vec{J}^{[2]}_{SRC}(i,j) = &-\frac{e_i}{2iM_N}\left[\vec{\nabla}_i\delta(\vec{r}-\vec{r}_i)+\delta(\vec{r}-\vec{r}_i)\vec{\nabla}_i\right]g(r_{ij})\\ &-\frac{e_j}{2iM_N}\left[\vec{\nabla}_j\delta(\vec{r}-\vec{r}_j)+\delta(\vec{r}-\vec{r}_j)\vec{\nabla}_j\right]g(r_{ij})\\ &-\frac{\mu_i e}{2M_N}\delta(\vec{r}-\vec{r}_i)\vec{\nabla}\times\vec{\sigma}_i g(r_{ij})\\ &-\frac{\mu_j e}{2M_N}\delta(\vec{r}-\vec{r}_j)\vec{\nabla}\times\vec{\sigma}_j g(r_{ij})\ . \end{aligned} \tag{53}$$

Similarly, the effective two-body charge density becomes :

$$\rho^{[2]}_{SRC}(i,j) = -\left(e_i\delta(\vec{r}-\vec{r}_i)+e_j\delta(\vec{r}-\vec{r}_j)\right)g(r_{ij})\ . \tag{54}$$

In order to facilitate the calculation of the matrix elements, the central correlation function is expanded according to :

$$g(r_{12}) = \sum_{lm}\frac{4\pi}{2l+1}g_l(r_1,r_2)Y^*_{lm}(\Omega_1)Y_{lm}(\Omega_2)\ . \tag{55}$$

The different partial-wave components can be directly obtained from :

$$g_l(r_1,r_2) = \frac{2l+1}{2}\int_{-1}^{+1}dx P_l(x)g\left(\sqrt{r_1^2+r_2^2-2r_1r_2x}\right)\ . \tag{56}$$

The expressions for the two-body transition matrix elements (20) and (21) with the effective two-body operators of Eqs. (53) and (54) are given in Appendix A. These matrix elements represent are at the basis of our calculation of the SRC contribution to exclusive (e,e′NN) and semi-exclusive (e,e′N) cross sections. Results of those calculations will be presented in the forthcoming sections. In the calculations which will be presented below we have used several forms of the central correlation function g. Theories that start from principal grounds, seem to produce correlation functions that are rather soft. In this context we refer to the Fermi Hypernetted Chain (FHNC) calculations of Refs. [3] and [44], the Monte Carlo calculations that were e.g. reported in Refs. [2] and [45] and the recent calculations performed in a translationally invariant framework [5]. The object of these studies is usually the ground-state properties of finite nuclear systems. Most of these calculations include also higher order cluster terms.

To set some kind of upper limit on the effect of the SRC for the calculated cross sections, we will also present results with a pronounced hard-core correlation function that is due to Ohmura, Morita and Yamada (OMY) [46] :

$$f(r) = \begin{cases} 0 & r \leq 0.6fm \\ [1 - \exp\left(-\mu^2(\mathrm{r}-\mathrm{c})^2\right)]\,[1 + \gamma \exp\left(\mu^2(\mathrm{r}-\mathrm{c})^2\right)] & r > 0.6fm \end{cases} , \quad (57)$$

with $\mu = 1.118\ fm^{-1}$ and γ=2.078. We do not consider this as a realistic correlation function but use this function to maximize the effect of the short-range correlations relative to the meson-exchange and Δ degrees of freedom.

3 Results and discussion

3.1 Exclusive (e,e′pp) and (e,e′pn) reactions

The most elementary (e,e′NN) cross sections (c.s.) that can be calculated are those for excitation of the residual nucleus in a specific (discrete) state. Even with fixed the electron kinematics, one is left with an angular cross section depending on five independent variables. An obvious choice for the latter are the two solid angles and one of the kinetic energies of the escaping particles : $(\Omega_a, \Omega_b, T_a)$. In what follows we will restrict ourselves to in-plane kinematics which fixes the azimuthal angle of the two detected nucleons at 0^o and 180^o degrees. In Figs. A.5 and A.6 we show ^{12}C(e,e′pp) and ^{12}C(e,e′pn) angular cross sections for creation of the final nucleus in a state with $\mid (1p_{3/2})^{-2}, J_R >$ two-hole structure and $J_R = 0^+$ and 2^+. The considered kinematical conditions are typical ones for the 800 MeV AMPS (Amsterdam) and MAMI (Mainz) electron accelerators. In order to further reduce the number of independent variables, for the calculations presented here we have considered the situation in which both escaping nucleons have equal kinetic energies at zero recoil momentum $\vec{p}_{A-2}$

$$\vec{p}_{A-2} = \vec{q} - \vec{k}_a - \vec{k}_b \ . \quad (58)$$

This means that the kinetic energy for one of the escaping particles was fixed at $T = (\omega - S_{2N})/2$, with S_{2N} the threshold energy for $2N$ emission. With this choice we are left with two independent variables, the polar angles of the escaping nucleons, against which the angular cross sections can be studied. In Figs. A.5 and A.6 the polar angles vary between 0^o and 360^o. Within this convention a typical back-to-back situation in the LAB frame would be e.g. $(\theta_a = 40^o, \theta_b = 220^o)$. The thresholds for proton-proton and proton-neutron

knockout from ^{12}C are respectively 27.2 and 27.4 MeV. Obviously, the two-nucleon knockout strength is residing in a very small part of the phase space, namely those situations in which both nucleons escape in an almost back-to-back situation. This type of behaviour can be easily explained by referring to the factorized model for two-nucleon knockout [13,47]. In such an approach it can be shown that the angular cross sections are proportional to the c.o.m. distribution $F(P)$ of the active nucleon pair. As the $F(P)$ is a sharply decreasing function with c.o.m. momentum $\mid \vec{P} \mid$ ($\vec{P} = -\vec{p}_{A-2}$), two-nucleon knockout will preferentially occur in those situations in which the momentum P is kept small. From energy-momentum conservation arguments, this corresponds with back-to-back emission. Despite the fact that in the unfactorized model some of the approximations which are at the basis of the factorization are not made, we still find the c.o.m. distribution of the pair to be a driving mechanism behind two-nucleon knockout. Besides this back-to-back dominance, it is clear that other variables do play a role. Inspecting Figs. A.5 and A.6 it is obvious that the angular momentum of the residual nucleus has a large impact on the shape of the angular cross section. The angular distributions for pp and pn knockout leading to a 2^+ state are much wider than those for the corresponding 0^+ state. Moreover, also the details of the leading photoabsorption mechanisms reflect themselves in the shapes of the angular cross sections. Even for creation of the final nucleus in a particular J_R and corresponding kinematical conditions, the proton-proton and proton-neutron cross section show some differences which can be related to the reaction mechanisms contributing to the cross sections. In this context, we want to remind the reader of the fact that the meson-exchange (Eq. (29)) and isobaric (Eq. (32)) currents have a peculiar isospin dependency which makes them behaving differently in the proton-proton and proton-neutron channel.

One of the main tasks of this paper is to investigate the sensitivity of the (e,e′NN) cross sections to dynamical short-range correlations. For that purpose we have calculated ^{16}O(e,e′pp) and (e,e′pn) angular cross section for emission out of the p-shell orbitals. A measure of the relative importance of the ground-state correlations in the whole reaction process, is the contribution from the longitudinal channel to the differential cross sections. Indeed, into first order the longitudinal channel is free from isobaric and meson-exchange current contributions. In the presented model calculations the longitudinal strength is exclusively the result of the existence of dynamical short-range correlations. A measure for the degree of longitudinal polarization of the virtual photon is the parameter ϵ_L

$$2\epsilon_L \equiv \frac{v_C}{v_T} = \left(tg^2 \frac{\theta_e}{2} - \frac{q_\mu q^\mu}{2 \mid \vec{q} \mid^2} \right)^{-1} . \tag{59}$$

In Figs. A.7-A.10 we have plotted some corresponding proton-proton and proton-neutron knockout angular cross sections at two values of the energy transfer. These have been chosen as to probe a kinematical regime well below and above the Δ resonance region (the equivalent photon energies K are 198 and 352 MeV respectively). The large incident electron energy (ϵ=1.2 GeV) and small electron scattering angle (θ_e=12 ^{o}) considered make the longitudinal polarization ϵ_L of the virtual photon large. For the results of Figs. A.7-A.10, we have considered the situation in which the residual nuclei ^{14}C and ^{14}N are created in a $\mid (1p_{3/2})^{-1}(1p_{1/2})^{-1}; J_R = 2^+ >$ state. According to the nuclear-structure calculations of Ref. [22] this type of configuration would be preferentially populated in ^{16}O(e,e$'$pp) reactions. Furthermore, we have considered the situation in which both escaping nucleons have the same kinetic energy at $\mid \vec{p}_{A-2} \mid = 0$. The proton-neutron channel is obviously a much stronger channel than the proton-proton emission channel. Inspecting Figs. A.8 and A.10 it is clear that proton-neutron emission is dominated by the transverse channel and that central ground-state correlations play only a marginal role.

The weaker proton-proton emission channel exhibits a stronger sensitivity to the ground-state correlations. Over the whole, however, the isobaric currents dominate the angular cross sections. There are some parts of the phase space, however, for which the longitudinal cross section is a sizeable contribution in the full cross section, reflecting the sensitivity of the reaction to ground-state correlation effects. The latter are e.g. playing a major role for kinematical conditions that correspond with one of the escaping nucleons moving along the direction of the three-momentum transfer $\vec{q}$.

All of the previous angular (e,e$'$NN) cross sections have been obtained with the central FHNC correlation function. The latter is of the Gaussian type $g(r_{12}) = \alpha e^{-\beta r_{12}^2}$. For ^{16}O, the parameters were calculated to be α=0.53 and β=1.52 fm^{-2} [3]. For our purposes, the parametrization for ^{12}C was assumed to be identical to the one for ^{16}O.

We now aim at studying the sensitivity of the calculated (e,e$'$pp) cross sections to the choice of the Jastrow correlation function. To this end, we do not longer consider the situation in which the residual nucleus is created in a particular J_R but plot the cross section which is obtained after (incoherently) adding all possible final angular momenta J_R. The number of situations which have to be considered depends on the quantum numbers $(l_h j_h, l_{h'} j_{h'})$ of the orbits from which the nucleons are escaping. For example, for proton-proton emission out of the $(1p_{3/2}, 1p_{1/2})$ orbits the plotted cross section is obtained after adding the contribution from $J_R = 1^+$ and 2^+. For the results of Fig. A.12 we consider the so-called coplanar and symmetrical situation. This type of kinematics has been schematically sketched in Fig. A.11 and corresponds with the situation in which both nucleons are escaping with equal kinetic energy and opening angle with respect to the direction of the transferred momentum. In

Fig. A.11 we show also the typical behaviour of the c.o.m. momentum P in such kinematics. So given the dominance of the c.o.m. distribution in producing the general features of the two-nucleon knockout cross sections, one would expect the angular cross section to peak around an opening angle of 70 degrees and fall off quickly to smaller and larger opening angles. This is precisely what is observed in Fig. A.12. Another observation is that with the central correlation function of Ref. [2], which is obtained with Monte-Carlo techniques, the Jastrow correlations are hardly affecting the differential cross sections that are obtained when solely accounting for the Δ degrees of freedom. In the remainder of the paper, the correlation function of Ref. [2] will be referred to as "MC". A more pronounced effect is found with the Gaussian FHNC correlation function. The short-range contribution is further noticed to depend on the single-particle levels from which the protons are escaping. Whereas the Gaussian FHNC correlation function slightly increases the cross sections for $(1p1/2)^{-2}$ and $(1p3/2)^{-2}$ knockout, the effect is quite sizeable for 2N knockout out of the mixed $(1p1/2)^{-1}(1p3/2)^{-1}$ orbits. The most spectacular shell dependence is noticed for the hard-core OMY correlation function. Counting the number of possible proton-proton pairs one would expect the absolute cross sections for the different two-hole configurations of Fig. A.12 to be like 6 $((1p3/2)^{-2})$:8 $((1p3/2)^{-1}(1p1/2)^{-1})$:1$((1p1/2)^{-2})$. It is obvious that the number of pairs can only serve as a rough guide to predict the relative amount of strength that goes into the different two-hole combinations.

In Fig. A.13 the four terms (longitudinal, transverse, longitudinal-transverse and transverse-transverse) contributing to the ^{16}O(e,e′pp)$((1p3/2)^{-1}(1p1/2)^{-1})$ angular cross sections of Fig. A.12 are shown for different choices of the central correlation function. It is clear that the absolute magnitude of the cross section is dominated by the transverse (T) and transverse-tranverse (TT) terms that show very little sensitivity to the central correlation effects. The longitudinal (L) and longitudinal-transverse (LT) structure functions, on the other hand, exhibit a very strong sensitivity to the choice of the correlation function. The hard-core OMY correlation function produces longitudinal (e,e′pp) strength that is typically one order of magnitude larger than the strength generated by the (realistic) soft-core MC and FHNC correlation functions. Remark further that the MC and FHNC correlation functions produce remarkably different L and LT structure functions. This is a rather surprising result as their functional dependence on the relative coordinate of the two interacting particles is rather similar.

3.2 Semi-exclusive (e,e′p)

In the plane-wave impulse approximation (PWIA) the (e,e′p) cross section can be cast in the form

$$\frac{d^4\sigma}{d\epsilon' d\Omega_{e'} d\Omega_p dE_p} = Ep\sigma_{ep} P(|\vec{p}_m|, E_m) \ , \tag{60}$$

where E_p (p_p) is the energy (momentum) of the detected proton and σ_{ep} the elementary cross section for electron scattering off an off-shell proton. It should be noted that a similar type of factorization can be pursued for the (γ,p) reaction. The spectral function $P(|\vec{p}_m|, E_m)$ is related to the probability of removing a nucleon with momentum p_m from the target nucleus and finding the residual nucleus at a missing energy E_m. The spectral function is of fundamental importance for the understanding of the many-body dynamics of finite nuclei and has been the subject of many theoretical considerations [42,48,49]. Eventhough a wide variety of spectral functions is available in literature, most calculations point towards the IPM providing a fair description of $P(k, E)$ at low k and E. As far as the spectral function is concerned, the deviations from the IPM model are predicted to occur at high energy and momentum. As a consequence, when trying to access these correlation effects with the aid of (e,e′p) measurements, one has to probe high missing energies, where the exclusive nature of the reaction can no longer be guaranteed. In this missing-energy range, the usefulness of the factorized cross section (60) becomes questionable. Indeed, contributions from genuine two-body photoabsorption, like e.g. those mediated by pion exchange, to the (e,e′p) cross section cannot be related to the single-particle spectral function, even when adopting a plane wave description for the escaping particles. On the other hand, one-body photoabsorption with subsequent emission of two nucleons is a signature of ground-state correlations and has also been predicted to be the major mechanism [8] feeding the high-momentum components in $P(k, E)$. Or put in other words, just as for the (e,e′NN) reaction, meson-exchange and isobaric currents are considered as unwanted noise when embarking on studies that aim at probing ground-state correlations with the semi-exclusive (e,e′p) and (γ,p) reaction.

In order to study the q-dependence of the semi-exclusive proton knockout channel we have gathered in Fig. A.14 a number of ^{12}C spectra that have been obtained for an energy transfer of about 200 MeV. The data include both real and virtual photon results and are obtained at several labs. A striking feature of the data is the ratio of the continuum strength ($E_m \geq 30$ MeV) to the strength residing in the discrete part of the spectrum. For the real photon case the continuum strength dominates the spectrum. For the highest momentum transfer considered here (q=585 MeV) the strength for one-nucleon removal from the 1p and 1s shell is clearly showing up. The real photon data do not

show any obvious indication for one-proton emission from the 1s-shell and the strength rises clearly beyond the two-particle emission threshold. An interesting case is the virtual photon spectrum that was obtained at low momentum transfer (q=270 MeV). Here the strength is a rather flat distribution that extends into the region of s-shell removal without reflecting a clear bump. Also shown in Fig. A.14 is the calculated contribution from proton-proton and proton-neutron emission to the semi-exclusive spectrum. These calculations have been performed according to the formalism outlined in Sect.2.2 and include the meson-exchange and isobaric currents in addition to the strength generated by the Jastrow correlations. The latter are accounted for in the FHNC parametrization. Apart from the highest momentum transfer considered here, the calculations give a reasonable account of the measured strength. The major contribution to the semi-exclusive spectrum is ascribed to proton-neutron knockout. This channel is predominantly fed by the meson-exchange and isobaric currents, which imposes some serious limitations on the suitability of the semi-exclusive reaction to probe ground-state correlations. Referring to Fig. A.14, it should be noted that the data taken at q=270 MeV are probing the dip region, whereas at q=585 MeV one is facing quasi-elastic conditions. One could thus conclude that semi-exclusive $(\gamma^{(*)}, p)$ processes are reasonably well understood at the real photon point and in the dip region. The situation is however quite different in the quasi-elastic regime for which the origin of the continuum strength cannot be explained in terms of two-nucleon knockout.

For all four situations considered in Fig. A.14 only situation (c) exhibits some sensitivity to the Jastrow correlations. For the other three cases photoabsorption on the meson-exchange and Δ currents dominates the calculated two-nucleon knockout strength. Under the kinematical conditions of (c) data are available for proton escaping angles varying from 27 ^{o} up to 162 ^{o}. In Ref. [50], we have compared our (e,e′p) model predictions for the full range of proton angles. A selective sensitivity to dynamical SRC was observed. The qualitative behaviour of this sensitivity could be explained within the context of the two-nucleon correlation model [8] that predicts an increased sensitivity to SRC effects when the following relation between the missing energy and momentum is (approximately) obeyed

$$E_m \approx S_{2N} + \left\langle E_x^{hh'} \right\rangle + \frac{(A-2)p_m^2}{2(A-1)M_N} \ , \tag{61}$$

where $\left\langle E_x^{hh'} \right\rangle$ is the average excitation energy of the $A-2$ system if the nucleons are escaping from the orbits characterized by h and h'. Apart from some factors that are related to recoil effects, the above relation reflects a picture in which correlated nucleons occur in pairs with respective momenta $\vec{p}_m$ and $-\vec{p}_m$. The kinematical conditions of the four situations considered in Fig. A.14 are shown in an (E_m, p_m) graph in Fig. A.15. The shaded region

is the area for which the above prescription (61) would predict an increased likelihood to detect ground-state correlation effects. The width of the shaded region was obtained by assuming that $0 \leq \left\langle E_x^{hh'} \right\rangle \leq 50\ MeV$, thus covering knockout from the $(1p)^2$, (1p)(1s) and $(1s)^2$ orbitals in ^{12}C. It was further assumed that correlation effects only occur for $p_m \geq 300\ MeV/c$. Despite the fact that some likelihood to observe SRC effects is predicted for the real-photon cases (a) and (b), the transverse character of the reaction makes the two-body currents dominating. For the situation (c) a proper balance between the longitudinal/transverse degrees of freedom and the condition (61) seems to be reached.

A possible way of learning more about the short-range correlations is the separation of the different (e,e′p) structure functions. In particular, the longitudinal response function opens good perspectives in that respect. As explained in Sect. 2.3, in lowest relativistic order the pion exchange effects are not affecting the longitudinal channel. For finite nuclei, only one experiment that separates the different structure functions in the high missing-energy region has been reported. In Ref. [54] the ^{12}C(e,e′p) structure functions have been separated in parallel kinematics ($\vec{p}_p \parallel \vec{q}$). Parallel kinematics is quite favourable for these purposes as only two structure functions (W_T and W_L) are contributing. The data of Ref. [54] are shown in Fig. A.16 and are characterized by an excess strength in the transverse response function in the missing energy region above the s-shell peak. The transverse (R_T) and longitudinal (R_L) structure functions of Fig. A.16 are obtained by dividing the longitudinal (transverse) part of the (e,e′p) cross section by $\sigma_M v_C$ ($\sigma_M v_T$). We have investigated in how far the observed excess strength in the transverse channel can be attributed to photoabsorption on correlated nucleon pairs with emission of two nucleons. In these calculations we have included the absorption mechanisms related to the SRC, IC and MEC. As becomes clear from Fig. A.16, the present model cannot account for the excess transverse strength. Remark that in the presented model calculations all two-nucleon emission strength in the longitudinal channel is attributed to short-range effects.

As we find that two-nucleon knockout cannot explain the excess transverse strength at high missing energies, we have investigated in how far single-nucleon knockout from the deep-lying shells could be at the origin of the different missing-energy behaviour in the longitudinal and transverse channel. For that purpose we have calculated the cross section for knockout from the $1s_{1/2}$ orbit at various values of T_p, covering the whole missing-energy range of the data. These calculations were done in a direct knockout model including both one- and two-body currents in the initial photoabsorption process [55]. For the whole missing-energy range covered here ($E_m \leq 70$ MeV) we use the bound state $1s_{1/2}$ wave function as obtained from a HF calculation. Formally, this means that in the calculations the spectral function

$$P_{lj}(k,E) = \sum_n \mid \left\langle \psi_n^{A-1}(E_n^{A-1}) \mid c_{ljk} \mid \psi_o(E_o^A \right\rangle \mid^2 \times \delta\left(E - \left(E_n^{A-1} - E_o^A\right)\right) \ , \tag{62}$$

is used in a factorized form :

$$P_{lj}(k,E) = \mid \phi_{lj}(k) \mid^2 S_{lj}(E)(2j+1) \ . \tag{63}$$

The function S_{lj} describes the spreading of the hole strength characterized by the quantum numbers lj as a function of the missing energy in the A-1 system

$$S_{lj}(E) = \sum_n \left| \left\langle \psi_n^{A-1}(E_N^{A-1}) \mid c_{lj} \mid \psi_o(E_o^A) \right\rangle \right|^2 \delta\left(E - \left(E_n^{A-1} - E_o^A\right)\right) \ , \tag{64}$$

and $\phi_{lj}(k)$ is the mean-field single-particle wave function in momentum space. Microscopic calculations of the single-particle spectral function [9], however, show that deviations from mean-field wavefunctions predominantly occur at higher missing energies ($E_m \geq 50$ MeV). As such, the factorized prescription (64) could be considered as a reasonable approximation as long as relatively low missing energies are probed. In order to account for the spreading of the 1s hole strength in ^{11}B we rely on a prescription which is due to Jeukenne and Mahaux [56]. In this parametrization the nucleon hole spectral function is determined by a Lorentzian with an energy-dependent width $\Gamma(E)$:

$$S_{lj}(E) = \frac{1}{2\pi} \frac{Z_{lj}\Gamma(E)}{\left(E - |\epsilon_{lj}|\right)^2 + \frac{1}{4}\left(\Gamma(E)\right)^2} \ , \tag{65}$$

where Z_{lj} (ϵ_{lj}) is the quasi-particle strength (energy) of the hole state under consideration. The width $\Gamma(E)$ is then related to the imaginary part W of the optical potential ($\Gamma = 2W$) for which the following parametrization is adopted

$$W(E) = \frac{9.(E - S_N)^4}{(E - S_N)^4 + (13.27)^4} \ \ (\text{MeV}) \ . \tag{66}$$

With the above assumptions a fair description of the missing-energy dependence is reached for the longitudinal (e,e′p) results shown in Fig.A.16. It is worth mentioning that the fact that the 1s strength has a high missing energy tail can be attributed to correlation effects. In order to reach the agreement of Fig.A.16 a spectroscopic factor of 0.5 for the 1s1/2 state has been adopted. Despite the reasonable description of the longitudinal structure function, the transverse strength remains underestimated over the whole missing energy range. Final-state interactions are a possible explanation for this observation. Eventhough differences in the way FSI affects the different response functions

have been noted, the FSI effects are unlikely to act in such a selective manner that they produce a long tail of strength in the transverse response function leaving the longitudinal one almost unaffected.

In Fig. A.17 we show a similar theoretical analysis for the measurements of Ref. [53] that were performed at higher energy and momentum transfer. The ^{12}C(e,e′p) data of Fig. A.17 refer to quasi-elastic conditions and were obtained in parallel kinematics ($\vec{p}_p \| \vec{q}$). As the data cover a larger missing-energy range than those of Ref. [54] the approximation (63) is at stake. The data show a clear bump in the missing-energy region that is dominated by proton removal out of the 1s-shell. Above the s-shell region, the data exhibit a long tail. Part of this strength can be attributed to two-nucleon knockout. For the largest momentum transfer considered here, however, the calculated two-nucleon knockout strength is just a small fraction of the measured strength. At q=585 MeV/c a reasonable account of the data is achieved when adding the calculated 2N knockout strength to the contribution related to knockout from the 1s shell. In the region just above the 1s bump where the approximation (63) is expected to be reasonable, the calculations underestimate the data in both cases. It remains to be investigated whether model calculations starting from realistic spectral functions can explain the origin of this strength.

4 Conclusion

In this paper we have provided a framework in which the effect of ground-state correlations on electroinduced one- and two-nucleon knockout cross sections could be quantified. We have gone beyond the standard shell-model by considering short-range corrections to the nuclear wave functions. In the first-generation calculations presented here, this has been achieved by a state-independent Jastrow ansatz. The effect of the short-range effects on the cross sections is estimated on the basis of a cluster expansion. It is shown that when considering correlated wave functions, standard one-body photoabsorption in the Impulse Approximation generates a whole chain of "effective" absorption mechanisms that are 2,3,..., A-body in nature. These multi-body effects can be related to the ground-state correlations and compete with regular two-nucleon photoabsorption mechanisms, as e.g. generated through meson-exchange and Δ_{33} creation.

In the model outlined, a partial-wave expansion technique is adopted for the description of the final-state interaction in A(e,e′NN) processes. A direct knockout reaction model is adopted. Special care is taken to treat all spin degrees of freedom and anti-symmetrization effects exactly. The model is particularly suited to calculate exclusive A(e,e′NN) angular cross sections for creation of the residual nucleus in a specific state.

A novel technique to calculate the 2N knockout contribution to the semi-exclusive (e,e′N) channel is outlined. With the aid of Racah algebra, the integration over the solid angle of the undetected escaping nucleon could be done analytically. This procedure cuts severely on the amount of numerical integrations which have to be performed. The procedure of calculating the semi-exclusive (e,e′p) strength adopted here, has the advantage of being unfactorized in nature. This allows calculating the contribution from ground-state correlations without excluding contributions from other sources, as e.g. these arising from photoabsorption on two-body currents. Such contributions are completely excluded when expressing the semi-exclusive (e,e′p) cross section in terms of the one-body spectral function.

As far as the exclusive 2N knockout channel is concerned, the numerical results presented here include both (e,e′pp) and (e,e′pn) angular cross sections for the target nuclei ^{12}C and ^{16}O. The shapes and magnitudes of the angular cross sections reflect the complexity of the photoabsorption mechanism and the shell-model structure of the target and residual nucleus. The (e,e′pn) channel is characterized by considerably larger cross sections than the (e,e′pp) channel. Electroinduced proton-neutron emission is dominated by the mesonic and Δ-isobar degrees of freedom, with the central ground-state correlations playing only a marginal role. Therefore, the proton-neutron knockout strength is predominantly transverse in nature even when longitudinal kinematics is adopted. Two-proton knockout, on the other hand, exhibits a selective sensitivity to ground-state correlation effects. A major source of electroinduced two-proton knockout is, however, the $\Delta N \rightarrow pp$ mechanism. It is therefore essential to have a realistic description of these isobar degrees of freedom. This requires the input of knowledge obtained within the context of pion and real-photon absorption on nuclei.

The conclusions drawn for the (e,e′NN) reaction have their implications for the semi-exclusive (e,e′p) channel as correlation effects will manifest themselves predominantly as two-nucleon knockout. The calculations predict this channel to be dominated by proton-neutron knockout, which in its turn is strongly fed through the meson-exchange and isobaric currents. Apart from the two-body currents considered here, also multi-scattering effects can contaminate the link between the semi-exclusive (e,e′p) data and the spectral function. This effect has been the object of several investigations [57,58] with sometimes different conclusions. All this puts heavy constraints on the applicability of the semi-exclusive (e,e′p) reaction to gain empirical information about the single-particle spectral function. In any case, the strength generated by meson-exchange and Δ degrees of freedom has to be carefully estimated and substracted from the (e,e′p) data before relating the measured strength to ground-state correlation effects. Better conditions to detect the correlation effects in (e,e′p) are predicted to occur at higher momentum transfer and specific bands in the (E_m, p_m) configuration space.

Acknowledgement
The authors are grateful to Dr. L.B. Weinstein for kindly providing the data files of the MIT measurements and stimulating discussions. This work has been supported by the Fund for Scientific Research-Flanders (FWO).

A Two-body matrix elements with short-range currents

The purpose of this Appendix is to give the expressions for the two-body matrix elements (Eqs. (21) and (20)) with the effective two-body currents that account for the short-range effects in the initial wave function (Eqs. (53) and (54)). As outlined in Sect. 2.4 these effective operators are composed of the one-body operators of the impulse approximation and a Jastrow like correlation function that corrects for short-range correlations in the initial-state wave function.

The longitudinal strength attributed to SRC is contained in the two-body charge density of Eq. (54) and is determined by the following effective Coulomb operator (17) :

$$M_{JM}^{coul}\left(\rho_{SRC}^{[2]}(1,2)\right) = -\Big(j_J(qr_1)Y_{JM}(\Omega_1)g(r_{12})e\frac{1+\tau_{z,1}}{2} + j_J(qr_2)Y_{JM}(\Omega_2)g(r_{12})e\frac{1+\tau_{z,2}}{2}\Big) \tag{A.1}$$

With the aid of the expansion (55) this leads to the following two-body matrix elements :

$$\begin{aligned}
&< ab; J_1 \| M_J^{coul}(\rho_{SRC}^{[2]}(1,2)) \| cd; J_2 > = \\
&-\sum_{lL} \sqrt{4\pi} e \frac{\widehat{J_1}\widehat{L}\widehat{J_2}}{\widehat{l}} < l\ 0\ L\ 0 \mid J\ 0 > \int dr_1 \int dr_2 g_l^c(r_1,r_2) \\
&\times[\delta_{ac,\pi}\ X(j_a,j_b,J_1;j_c,j_d,J_2;L,l,J)D(a,c,L,r_1)D(b,d,l,r_2)j_J(qr_1) \\
&+\delta_{bd,\pi}\ X(j_a,j_b,J_1;j_c,j_d,J_2;l,L,J)D(b,d,L,r_2)D(a,c,l,r_1)j_J(qr_2)]
\end{aligned} \tag{A.2}$$

with

$$D(a,b,l,r) \equiv < l_a j_a \| Y_l(\Omega) \| l_b j_b >_r \ . \tag{A.3}$$

The radial transition density $< a\|\widehat{O}\|b >_r$ is defined such that it is related to the full matrix element through $< a\|\widehat{O}\|b >= \int dr < a\|\widehat{O}\|b >_r$. In the above expressions X denotes the 9j symbol in the conventions of ref. [59] :

$$X(j_a,j_b,J_1;j_c,j_d,J_2;j_e,j_f,J) \equiv \left\{ \begin{array}{ccc} j_a & j_b & J_1 \\ j_c & j_d & J_2 \\ j_e & j_f & J \end{array} \right\} .$$

Introducing the operator

$$O^{\kappa}_{JM}(q) = \sum_{M_1,M_2} \int d\vec{r} < J+\kappa\ M_1\ 1\ M_2|J\ M > \\ \times Y_{J+\kappa M_1}(\Omega) j_{J+\kappa}(qr) J_{M_2}(\vec{r})\ , \tag{A.4}$$

the electric and magnetic transition operators (Eq. 16) can be rewritten as :

$$T^{mag}_{JM}(q) = O^{\kappa=0}_{JM} \tag{A.5}$$

$$T^{el}_{JM}(q) = \sum_{\kappa=\pm 1} \frac{i(-1)^{\delta_{\kappa,+1}}}{\widehat{J}} \sqrt{J+\delta_{\kappa,-1}} O^{\kappa}_{JM}\ . \tag{A.6}$$

Accordingly, the matrix elements of the operator O^{κ}_{JM} suffice to determine both the electric and the magnetic strength. The transverse strength attributed to SRC is determined by the effective two-body current of Eq. (53). The latter has two components related to the convection and magnetization one-body current of the impulse approximation. For the component related to the magnetization current the effective O^{κ}_{JM} operator reads :

$$O^{\kappa}_{J}\left(\vec{J}^{[2],magn}_{SRC}(1,2)\right) = -\int d\vec{r} \sum_{M_1 M_2} < J+\kappa\ M_1\ 1\ M_2 \mid JM > \\ \times \left\{ \frac{\mu_1 e}{2M_N} \delta(\vec{r}-\vec{r}_1) g(r_{12}) \left(\left(\vec{\nabla} \times \vec{\sigma}_1 \right)_{M_2} Y_{J+\kappa M_1}(\Omega) j_{J+\kappa}(qr) \right) \right. \\ \left. + \frac{\mu_2 e}{2M_N} \delta(\vec{r}-\vec{r}_2) g(r_{12}) \left(\left(\vec{\nabla} \times \vec{\sigma}_2 \right)_{M_2} Y_{J+\kappa M_1}(\Omega) j_{J+\kappa}(qr) \right) \right\} \tag{A.7}$$

After some lenghty but straightforward manipulations, the transition matrix element for this operator can be reduced to :

$$< ab; J_1 \| O^{\kappa}_{J}\left(\vec{J}^{[2],magn}_{SRC}(1,2)\right) \| cd; J_2 > = \sqrt{6\pi} \frac{ieq}{M_N} \\ \times \sum_{\eta=\pm 1} \sum_{lLJ_4} \frac{\widehat{J_1}\widehat{L}\widehat{J_2}\widehat{J}\widehat{J_4}}{\widehat{l}} < l\ 0\ L\ 0 \mid J+\kappa+\eta\ 0 > \\ \times \sqrt{J+\kappa+\delta_{\eta,+1}} \left\{ \begin{array}{ccc} J & 1 & J+\kappa+\eta \\ L & l & J_4 \end{array} \right\} \left\{ \begin{array}{ccc} J+\kappa & J+\kappa+\eta & 1 \\ 1 & 1 & J \end{array} \right\} \\ \times \int dr_1 \int dr_2 g^{c}_{l}(r_1,r_2) \left\{ [\mu_p \delta_{ac,\pi} + \mu_n \delta_{ac,\nu}] (-1)^{l+J+J_4} \right. \\ \times X(j_a, j_b, J_1; j_c, j_d, J_2; J_4, l, J) B(a, c, J+\kappa+\eta, L, J_4, qr_1) D(b, d, l, r_2) \\ + [\mu_p \delta_{bd,\pi} + \mu_n \delta_{bd,\nu}]\, X(j_a, j_b, J_1; j_c, j_d, J_2; l, J_4, J) \\ \left. \times B(b, d, J+\kappa+\eta, L, J_4, qr_2)] D(a, c, l, r_1) \right\}\ , \tag{A.8}$$

where we have introduced the radial transition density

$$B(a,b,l,J_1,J_2,pr) \equiv < a \| j_l(pr) \left[Y_{J_1}(\Omega) \otimes \vec{\sigma} \right]_{J_2} \| b >_r$$

$$= \widehat{j_a}\widehat{J_2}\widehat{j_b}X(l_a,1/2,j_a;l_b,1/2,j_b;J_1,1,J_2)\widehat{l_a}\widehat{J_1}\sqrt{\frac{3}{2\pi}}$$
$$\times(-1)^{J_1} < l_a\ 0\ J_1\ 0|l_b\ 0 > r^2\varphi_a(r)\varphi_b(r)j_l(pr)$$

The matrix element for the SRC contribution related to the convection current can be derived in an analoguous manner and reads :

$$< ab;J_1\|O^\kappa_J\left(\vec{J}^{[2],conv}_{SRC}(1,2)\right)\|cd;J_2 >=$$
$$\sqrt{\pi}\frac{e}{iM_N}\sum_{lLJ_4}\frac{\widehat{J_1}\widehat{J_2}\widehat{J}\widehat{J_4}\widehat{L}}{\widehat{l}} < l\ 0\ L\ 0\mid J+\kappa\ 0 >$$
$$\times\left\{\begin{array}{ccc} J & 1 & J+\kappa \\ L & l & J_4 \end{array}\right\}(-1)^{L+J_4}\int dr_1\int dr_2 g^c_l(r_1,r_2)$$
$$\times\{\delta_{ac,\pi}X(j_a,j_b,J_1;j_c,j_d,J_2;J_4,l,J)E(a,c,J+\kappa,L,J_4,qr_1)D(b,d,l,r_2)$$
$$+\delta_{bd,\pi}(-1)^{l+J_4+J}X(j_a,j_b,J_1;j_c,j_d,J_2;l,J_4,J)$$
$$\times E(b,d,J+\kappa,L,J_4,qr_2)D(a,c,l,r_1)\}\ , \qquad \text{(A.9)}$$

where we have introduced the radial transition density $E(a,b,l,J_1,J_2,pr)$

$$E(a,b,l,J_1,J_2,pr) \equiv < a\|j_l(pr)\left[Y_{J_1}(\Omega)\otimes(\vec{\nabla}-\vec{\nabla}')\right]_{J_2}\|b >_r\ . \qquad \text{(A.10)}$$

The notation $\vec{\nabla}'$ refers to a gradient operator acting to the left. The terms involving the derivates of the central correlation functions have been neglected in the above expression.

References

[1] C. Mahaux and R. Sartor, Adv. Nucl. Phys. **20** (1991) 1.

[2] S.C. Pieper, R.B. Wiringa and V.R. Pandharipande, Phys. Rev. **C46** (1992) 1741.

[3] G. Co′, A. Fabrocini, S. Fantoni and I.E. Lagaris, Nucl. Phys. **A549** (1992) 439.

[4] F. Dellagiacoma, G. Orlandini and M. Traini, Nucl. Phys. **A393** (1983) 95.

[5] R. Guardiola, P.I. Moliner, J. Navarro, R.F. Bishop, A. Puente and Niels R. Walet, Nucl. Phys. **A609** (1996) 218.

[6] A. Wirzba, H. Toki, E.R. Siciliano, Mikkel B. Johnson and R. Gilman, Phys. Rev. **C40** (1989) 2745.

[7] Mikkel B. Johnson, E.R. Siciliano and H. Sarafian, Phys. Lett. **B243** (1990) 18.

[8] C. Ciofi degli Atti and S. Simula, Phys. Rev. C **53** (1996) 1689.

[9] H. Mütter and W.H. Dickhoff, Phys. Rev. C **49** (1994) R17.

[10] L. Weinstein and W. Bertozzi, Proc. of the 6th Workshop on Perspectives in Nuclear Physics at Intermediate Energies, (ICTP-Trieste, Italy, May 3-7, 1993), Eds. S. Boffi, C. Ciofi degli Atti and M. Giannini, World Scientific (1994), 362.

[11] L.B. Weinstein and W. Bertozzi, *in* Proc. of the Fourth Workshop on Perspectives in Nuclear Physics at Intermediate Energies (Trieste, 1988), Eds. S. Boffi, C. Ciofi degli Atti and M. Giannini, (World Scientific, Singapore, 1989).

[12] V. Van der Sluys, J. Ryckebusch and M. Waroquier, Phys. Rev. C **49** (1994) 2695.

[13] Kurt Gottfried, Nucl. Phys. **5** (1958) 557.

[14] G.E. Cross *et al.*, Nucl. Phys. **A593** (1995) 463.

[15] P. Grabmayr *et al.*, Phys. Lett. **B370** (1996) 17.

[16] Th. Lamparter *et al.*, Z. Phys. **A355** (1996) 1.

[17] P.D. Harty *et al.*, Phys. Lett. **B380** (1996) 247.

[18] A. Zondervan *et al.*, Nucl. Phys. **A587** (1995) 697.

[19] L.J.H.M. Kester *et al.*, Phys. Rev. Lett. **74** (1995) 1712.

[20] J. Ryckebusch, M. Vanderhaeghen, L. Machenil and M. Waroquier, Nucl. Phys. **A568** (1994) 828.

[21] M. Waroquier, J. Ryckebusch, J. Moreau, K. Heyde, N. Blasi, S.Y. van der Werf and G. Wenes, Phys. Rep. **148** (1987) 249.

[22] W.J.W. Geurts, K. Allaart, W.H. Dickhoff, H. Müther, Phys. Rev. C **54** (1996) 1144.

[23] J. Ryckebusch, L. Machenil, M. Vanderhaeghen, V. Van der Sluys and M. Waroquier, Phys. Rev. **C49** (1994) 2704.

[24] R. Machleidt *in* Relativistic Dynamics and Quark-Nuclear Physics, Eds. M.B. Johnson and A. Picklesimer, (John Wiley and Sons, New York, 1986), 71.

[25] M. Vanderhaeghen, L.Machenil, J. Ryckebusch and M. Waroquier, Nucl. Phys. **A580** (1994) 551.

[26] E. Oset, H. Toki and W. Weise, Phys. Rep. **83** (1982) 281.

[27] M.J. Dekker, P.J. Brussaard and J.A. Tjon, Phys. Rev. C **49** (1994) 2650.

[28] B. Körfgen, P. Oltmanns, F. Osterfeld and T. Udagawa, Phys. Rev. C, (1997) in press.

[29] N. Bianchi *et al.*, Phys. Rev. C **54** (1996) 1688.

[30] J.K. Koch and N. Ohtsuka, Nucl. Phys. **A435** (1985) 765 and J. Koch *in* Moderns Topics in Electron Scattering, Eds. B. Frois and I. Sick, (World Scientific, Singapore) (1991) 28.

[31] J.S. O'Connell *et al.*, Phys. Rev. C **35** (1987) 1063.

[32] C.R. Chen and T.-S.H. Lee, Phys. Rev. C **38** (1988) 2187.

[33] I.J.D. MacGregor *et al.*, to be published.

[34] T. Wilbois, P. Wilhelm, and H. Arenhövel, Phys. Rev. C **54** (1996) 3311.

[35] J. Ryckebusch, L. Machenil, M. Vanderhaeghen, V. Van der Sluys, and M. Waroquier, Phys. Rev. C **54** (1996) 3313.

[36] D.O. Riska, in Prog. Part. and Nucl. Physics, Vol. 11 (1982) 199.

[37] M. Gaudin, J. Gillespie and G. Ripka, Nucl. Phys. **A176** (1971) 237.

[38] J.W. Clark, *in* The many-body problem : Jastrow correlations versus Brueckner Theory, R. Guardiola and J. Ros eds., Lecture Notes in Physics **138** (Springer Verlag, Berlin, 1981) 184.

[39] S. Fantoni and V.R. Pandharipande, Nucl. Phys. **A473** (1987) 234.

[40] Adelchi Fabrocini, Phys. Lett. **B322** (1994) 171.

[41] V.R. Pandharipande and R.B. Wiringa, Rev. Mod. Phys. **51** (1979) 821.

[42] A.N. Antonov, P.E. Hodgson and I. Zh. Petkov, Nucleon Momentum and Density Distributions in Nuclei (Clarendon Press, Oxford, 1988).

[43] J.W. Van Orden and T.W. Donnelly, Ann. of Physics **131** (1981) 451.

[44] G. Co′, A. Fabrocini and S. Fantoni, Nucl. Phys. **A568** (1994) 73.

[45] O.Benhar, A. Fabrocini and S. Fantoni, in *Modern Topics in Electron Scattering*, eds. B. Frois and I. Sick (World Scientific, Singapore, 1991), 460.

[46] T. Ohmura, M. Morita and M. Yamada, Prog. Theor. Phys. **15** (1956) 222.

[47] J. Ryckebusch, Phys. Lett. **B383** (1996) 1.

[48] I. Sick, S. Fantoni, A. Fabrocini and O. Benhar, Phys. Lett. **B323** (1994) 323.

[49] O. Benhar, A. Fabrocini, S. Fantoni and I. Sick, Nucl. Phys. **A579** (1994) 493.

[50] Jan Ryckebusch, Marc Vanderhaeghen, Kris Heyde and Michel Waroquier, Phys. Lett. **B350** (1995) 1.

[51] M. Anghinolfi *et al.*, Nucl. Phys. **A457** (1986) 645.

[52] L.J.H.M. Kester *et al.*, Phys. Lett. **B344** (1995) 79.

[53] L.B. Weinstein *et al.*, Phys. Rev. Lett. **64** (1990) 1646.

[54] P.E. Ulmer *et al.*, Phys. Rev. Lett. **59** (1987) 2259.

[55] V. Van der Sluys, J. Ryckebusch and M. Waroquier, Phys. Rev. **C54** (1996) 1322.

[56] J.P. Jeukenne and C. Mahaux, Nucl. Phys **A394** (1983) 445.

[57] T. Takaki, Phys. Rev. **C39** (1989) 359.

[58] I. Sick, preprint University of Basel.

[59] I. Talmi, Simple Models of Complex Nuclei : The Shell Model and Interacting Boson Model, (Harwood Academic Publishers, Chur, 1993).

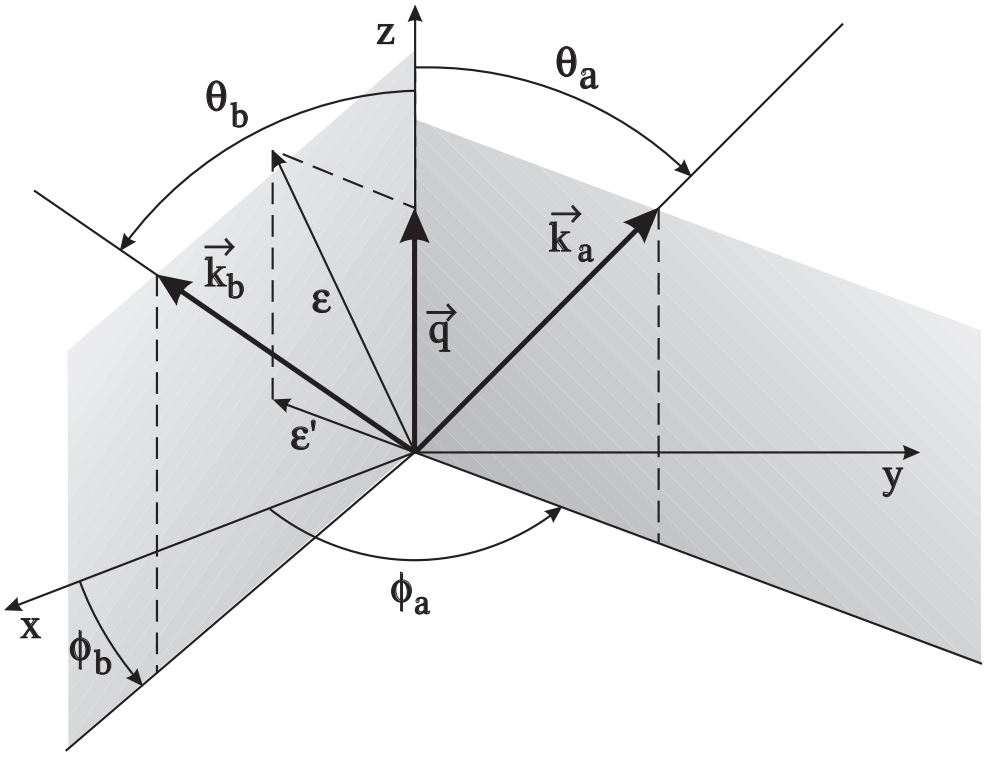

Fig. A.1. Adopted conventions for the angular variables of an A(e,e′$N_a N_b$) reaction. The electron scattering plane is the xz plane.

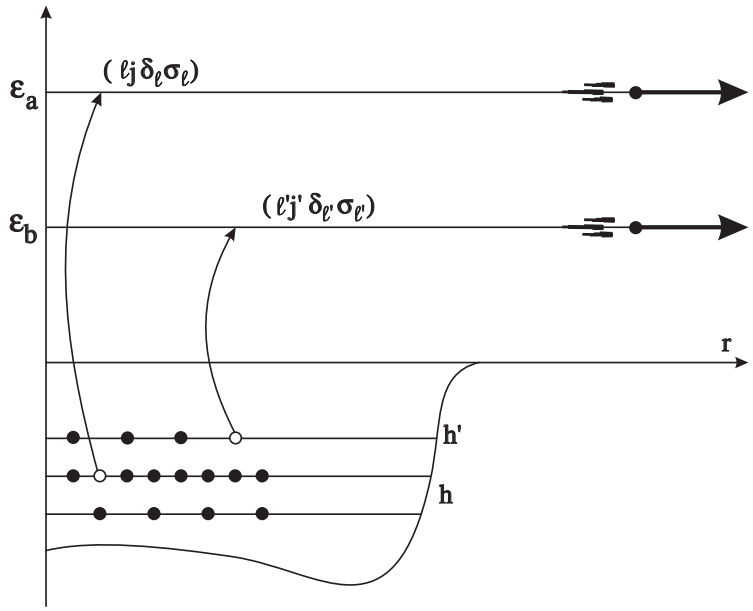

Fig. A.2. Two-nucleon knockout as interpreted in a shell-model picture. After ejection of two nucleons with energy ϵ_a and ϵ_b the residual nucleus is left in a two-hole state $(\mathrm{hh}')^{-1}$.

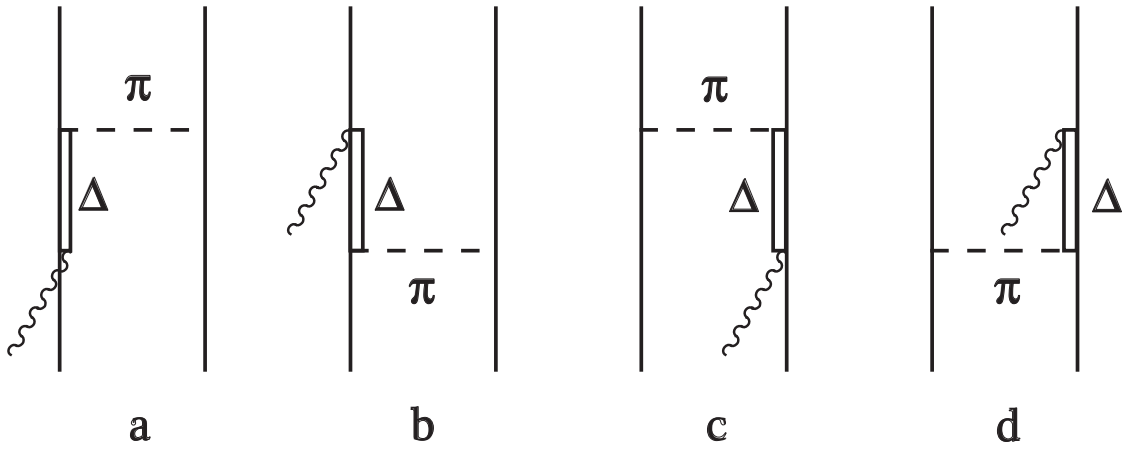

Fig. A.3. The four diagrams corresponding with Δ_{33} creation and π-exchange.

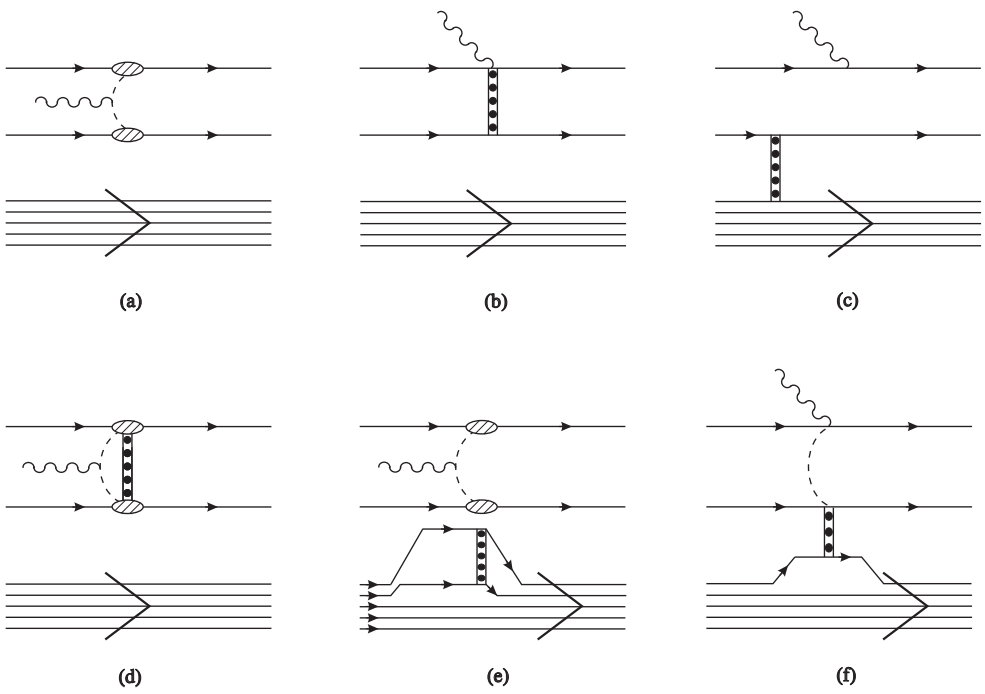

Fig. A.4. Different contributions to photoinduced two-nucleon knockout. Meson exchange processes are denoted with the dashed line. The photon is indicated with a wavy line and the ground-state correlations with the heavy dots.

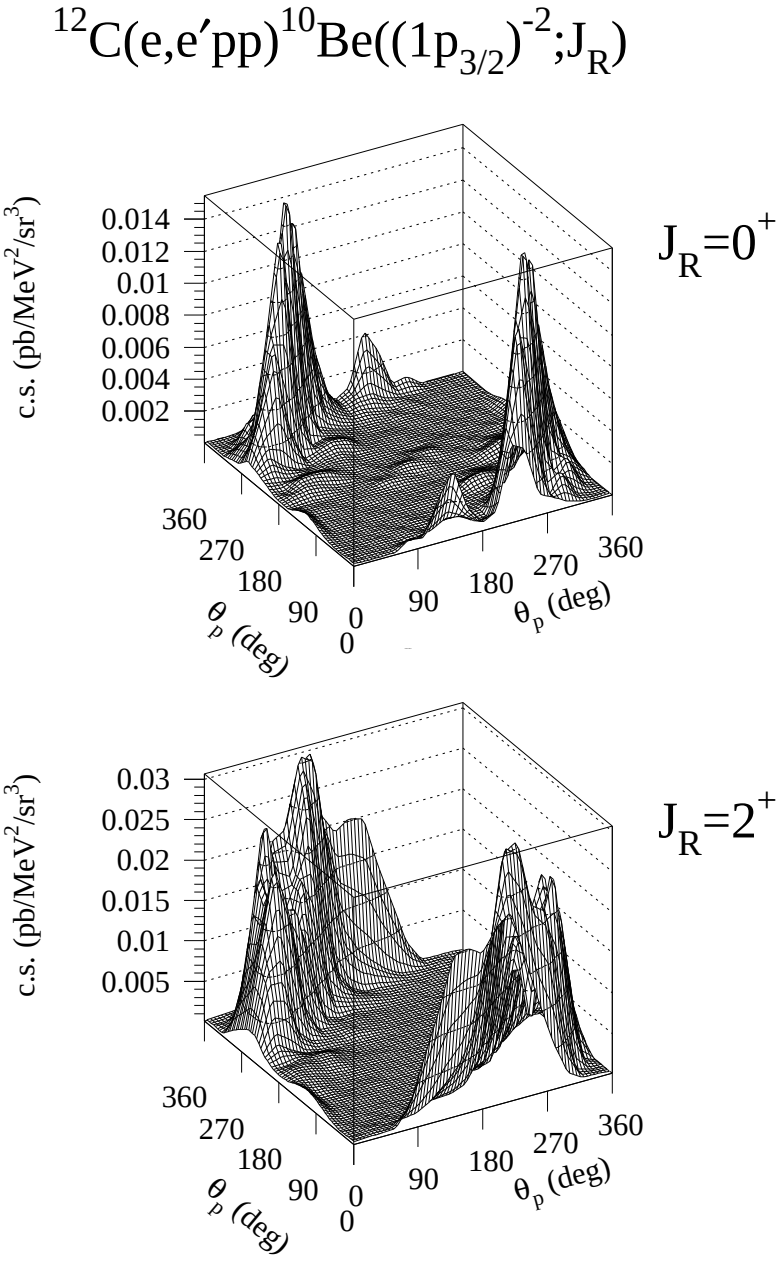

Fig. A.5. Differential cross sections for the ^{12}C(e,e′pp) reaction at ϵ=700 MeV, ω=250 MeV and θ_e=30^o (q=383 MeV/c) for excitation of an $\mid (1p_{3/2})^{-2}; 0^+ >$ and an $\mid (1p_{3/2})^{-2}; 2^+ >$ state respectively.

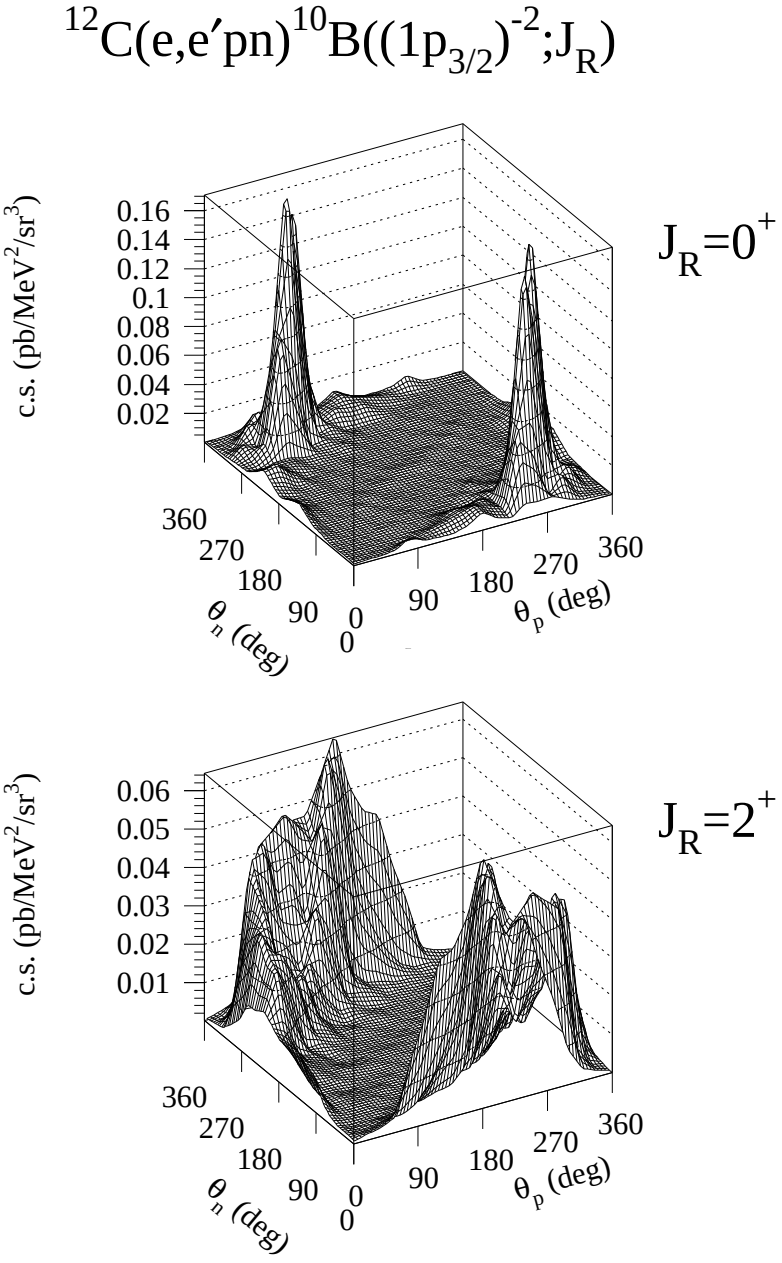

Fig. A.6. As in Fig. A.5 but now for the ^{12}C(e,e′pn) reaction

.

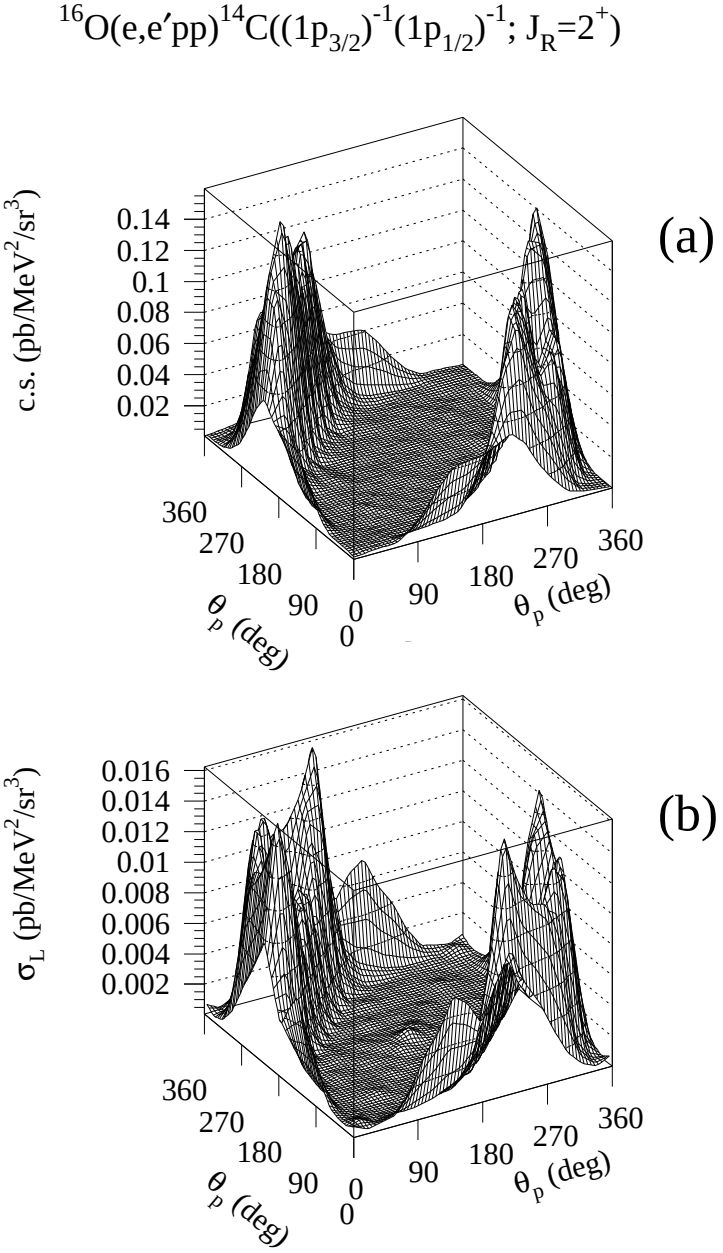

Fig. A.7. Differential cross sections for the ^{16}O(e,e′pp) reaction at ϵ=1.2 GeV, ω=225 MeV and θ_e=12^o (q=319 MeV/c) for excitation of an $|\,(1p_{3/2})^{-1}(1p_{1/2})^{-1}; J_R = 2^+ >$ two-hole state. (a) full cross section (b) longitudinal contribution.

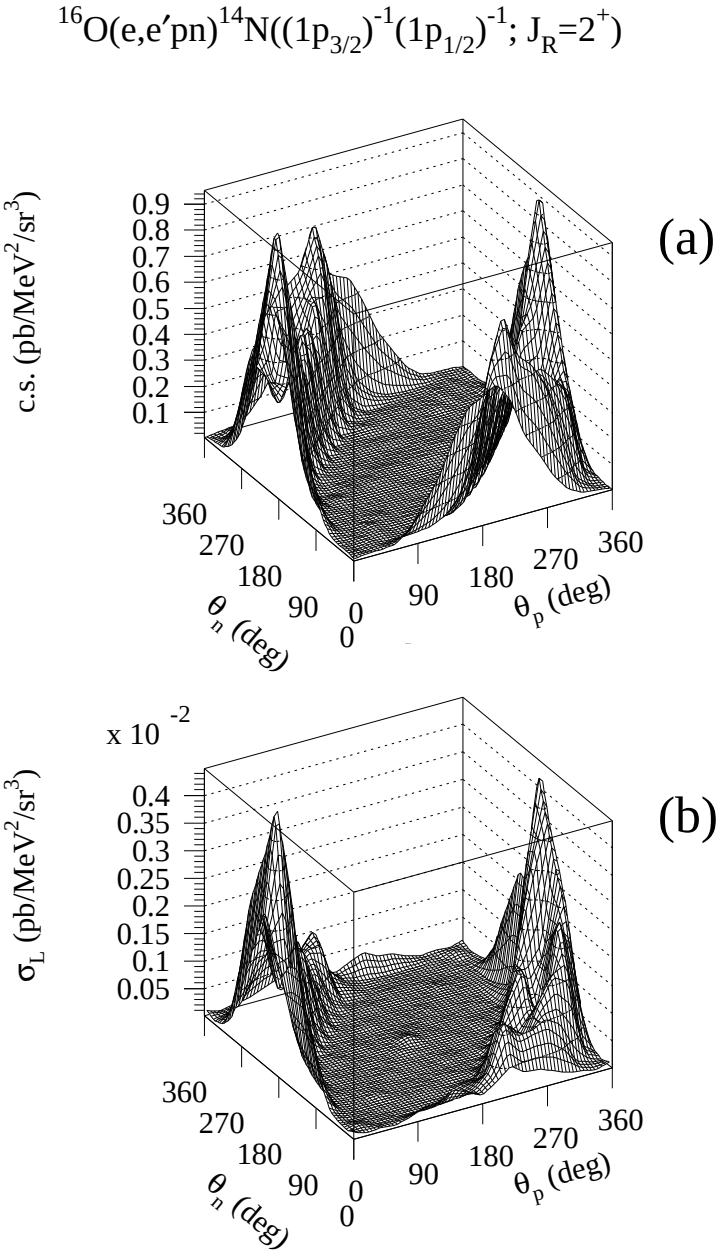

Fig. A.8. As in Fig. A.7 but now for proton-neutron emission.

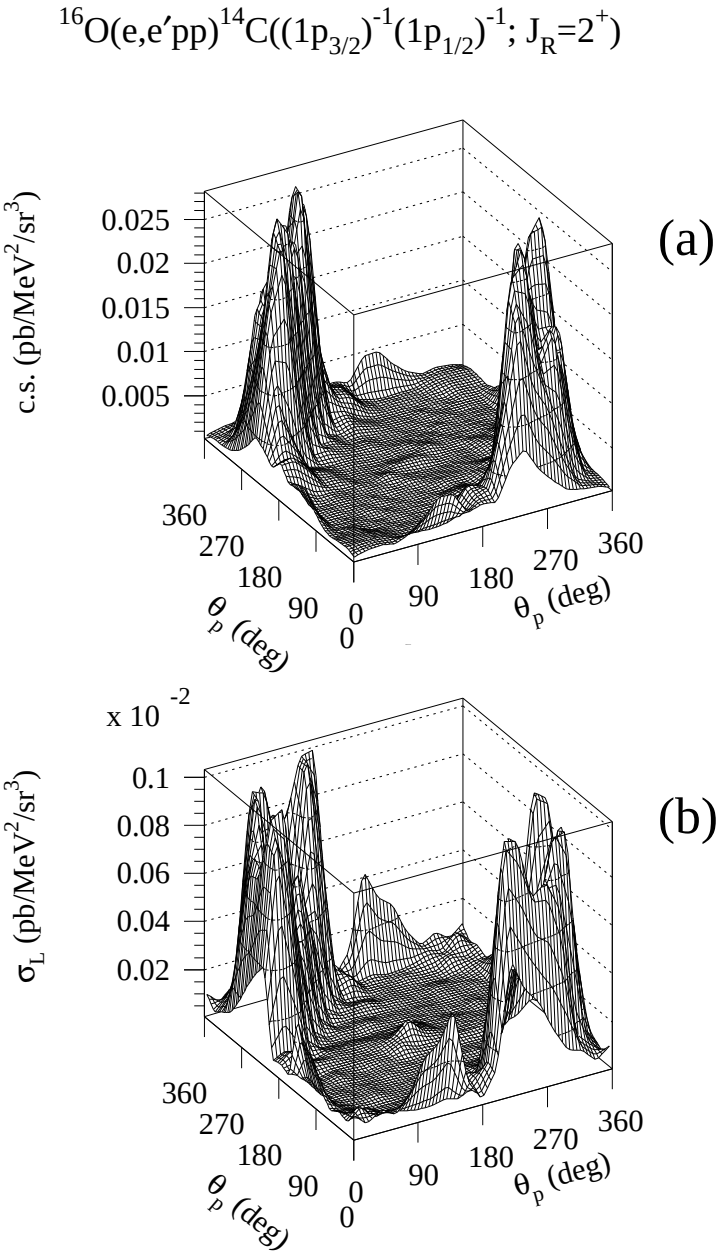

Fig. A.9. Differential cross sections for the ^{16}O(e,e′pp) reaction at ϵ=1.2 GeV, ω=375 MeV and θ_e=12^o (q=429 MeV/c) for the excitation of an $|\,(1p_{3/2})^{-1}(1p_{1/2})^{-1}; J_R = 2^+ >$ two-hole state. (a) full cross section (b) longitudinal contribution.

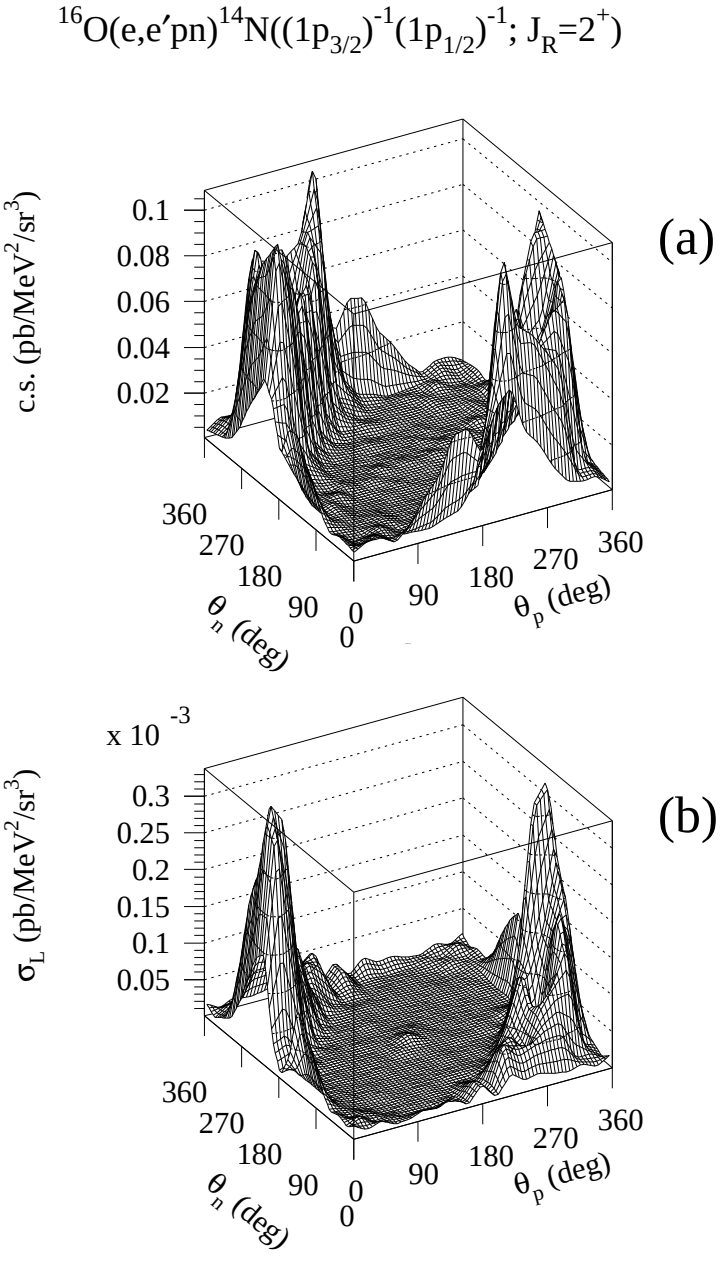

Fig. A.10. As in Fig. A.9 but now for proton-neutron emission.

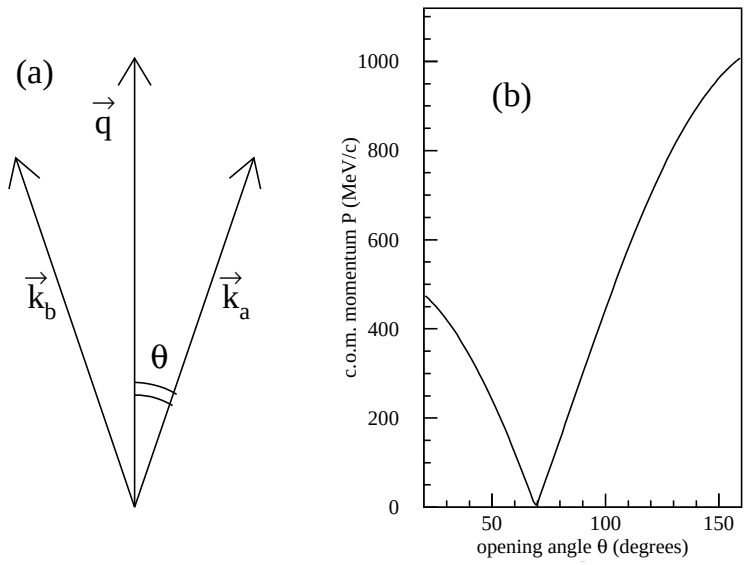

Fig. A.11. (a) Coplanar and symmetrical kinematics. (b) the c.o.m. momentum P as a function of the opening angle θ for two-proton knockout from ^{16}O at an energy transfer of ω=210 MeV.

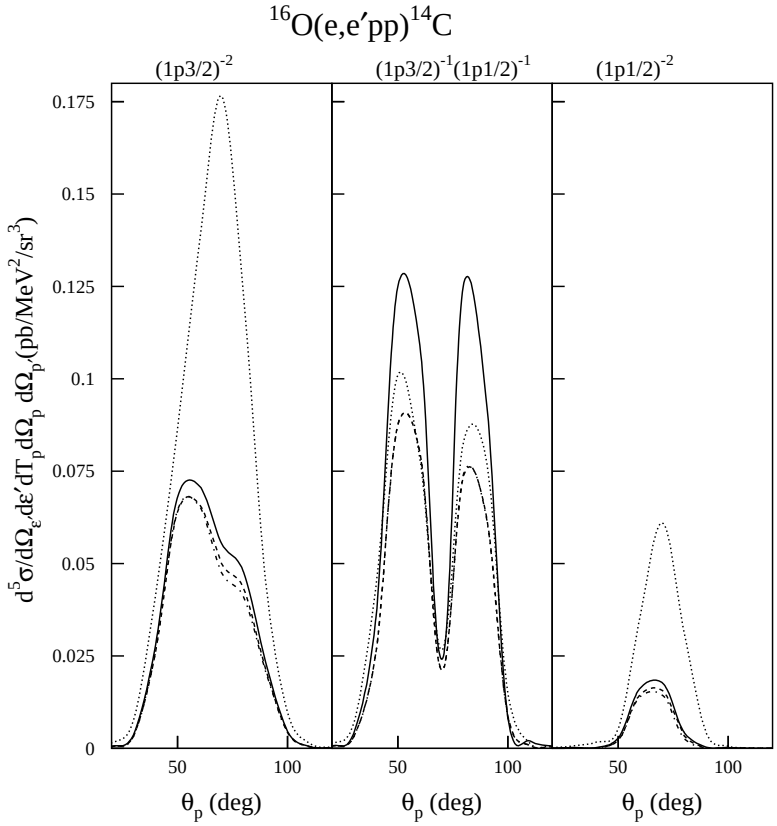

Fig. A.12. The ^{16}O(e,e′pp) differential cross section as a function of the proton angle in coplanar and symmetrical kinematics for ϵ=516 MeV, ω=210 MeV and θ_e=31^o. The different combinations for emission out of the p-shell orbits are considered. Different central correlation functions have been used : OMY (dotted line), FHNC (solid line) and MC (dashed line). The dot-dashed line is the result of a calculation in which only the isobaric currents are included.

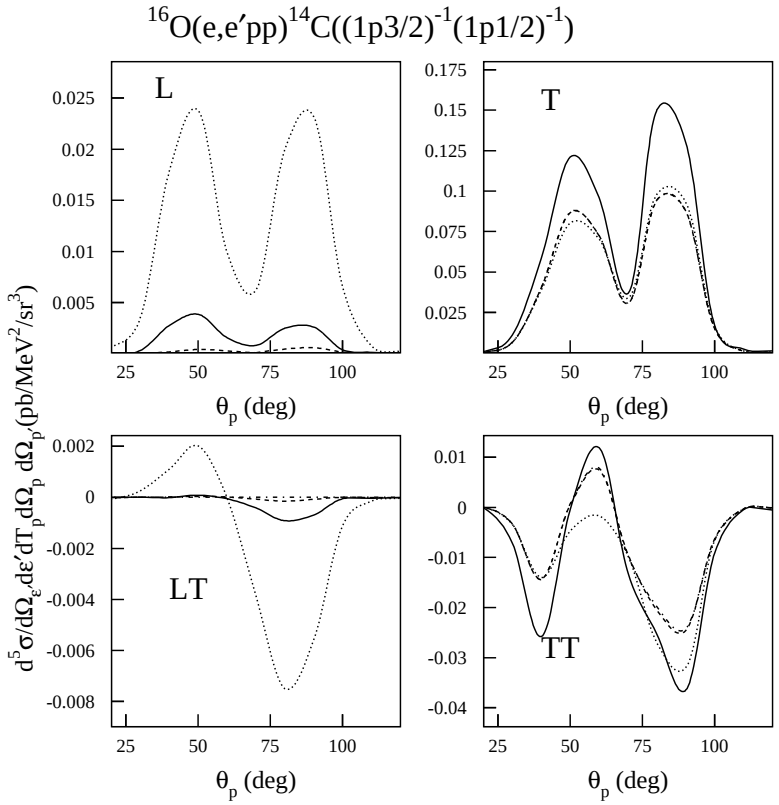

Fig. A.13. The four terms contributing to the ^{16}O(e,e′pp)$((1p3/2)^{-1}(1p1/2)^{-1})$ angular cross sections plotted in the central panel of Fig. A.12. The dot-dashed line shows the result when including only the delta-currents. The other curves are obtained after adding also the central short-range effects. Different central correlation functions have been used : OMY (dotted line), FHNC (solid line) and MC (dashed line).

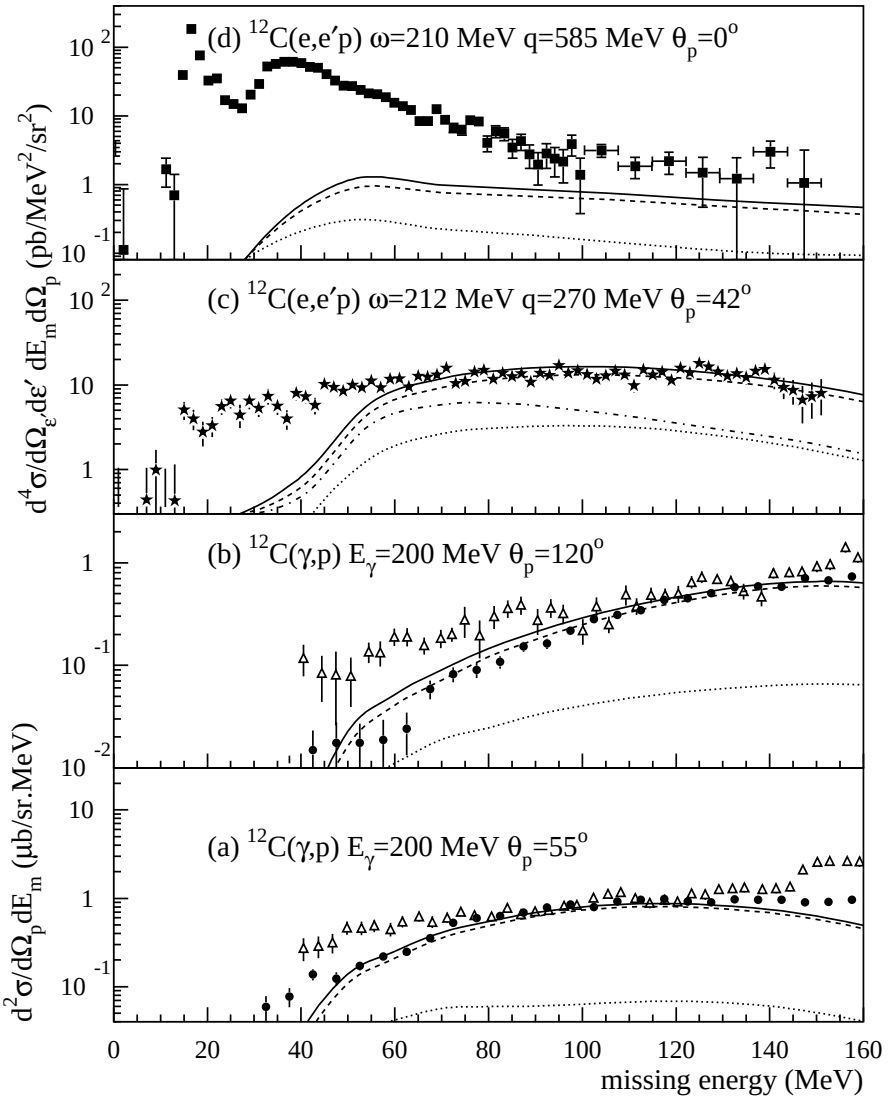

Fig. A.14. Missing-energy dependence of the semi-exclusive ^{12}C(e,e′p) and ^{12}C(γ,p) spectrum for $\omega \approx 200$ MeV and various kinematical conditions. The dotted (dashed) line shows the calculated contribution from proton-proton (proton-neutron) emission. The solid line is the incoherent sum of all the calculated strength contributions. The dot-dashed line is the calculated contribution from two-nucleon knockout including only the transverse two-body currents (for most cases this line falls on top of the solid one). The data are from Refs. [14] (circles), [53] (squares), [51] (triangles) and [52] (stars) .

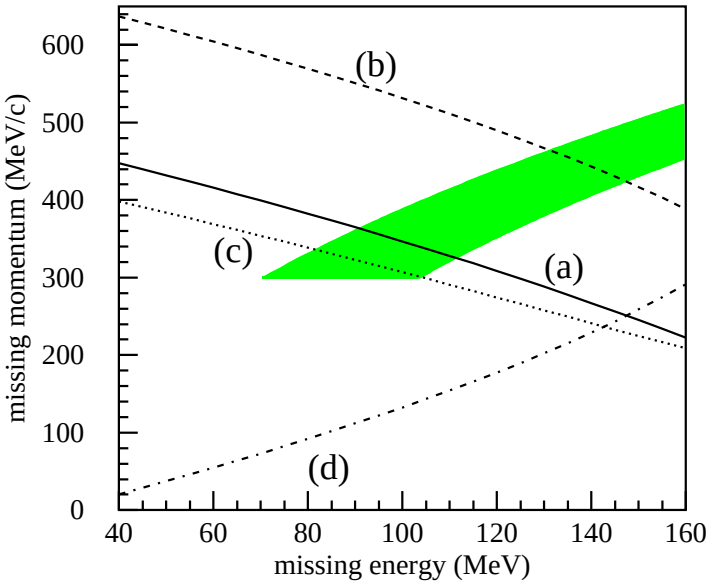

Fig. A.15. The missing momentum as a function of the missing energy for the kinematical conditions of Fig. A.14.

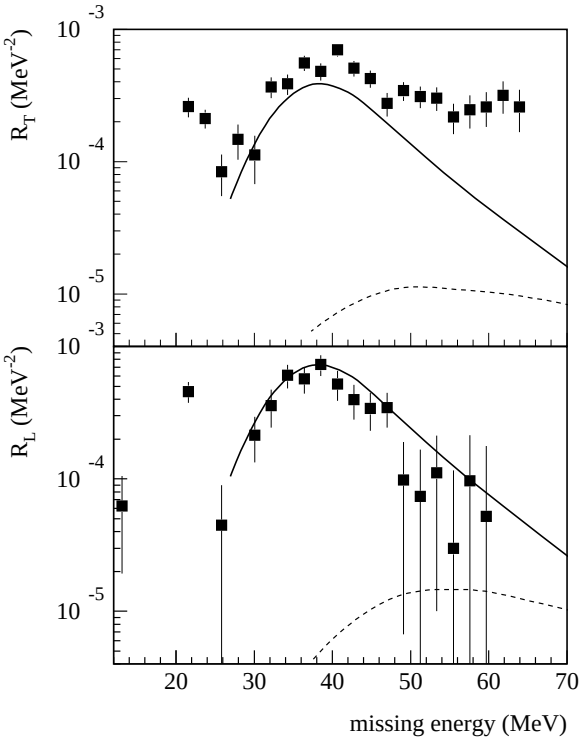

Fig. A.16. The longitudinal and transverse structure functions versus missing energy for the ^{12}C(e,e′p) reaction at ω=122.5 MeV and q=397 MeV/c. The dashed line is the calculated contribution from proton-proton and proton-neutron emission. The solid line is the predicted contribution for one-proton knockout from the 1s shell applying the same spectroscopic factor in the longitudinal and transverse structure function. The data are from Ref. [54].

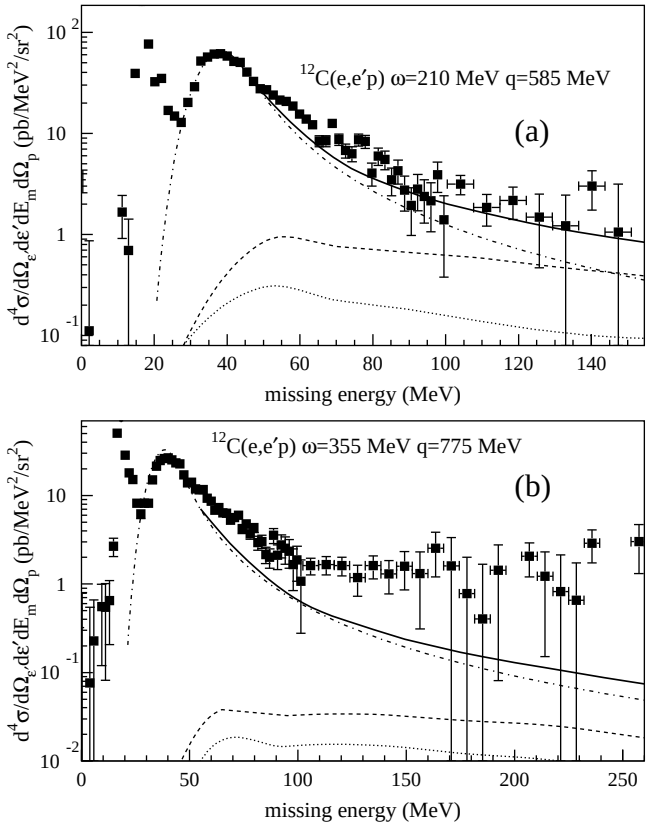

Fig. A.17. Missing-energy spectra for ^{12}C(e,e′p) at quasi-elastic kinematics. (a) ϵ=505.4 MeV, ω=210 MeV and q=585 MeV/c (b) ϵ=698 MeV, ω=355 MeV and q=775 MeV/c. The dotted (dashed) line is the calculated strength from (e,e′pp) ((e,e′pn)). The dot-dashed line the calculated strength from exclusive one-proton ejection out of the 1s shell. The solid is the summed strength from all calculated contributions. The data are from Ref. [53].